Recent changes in atmospheric methane

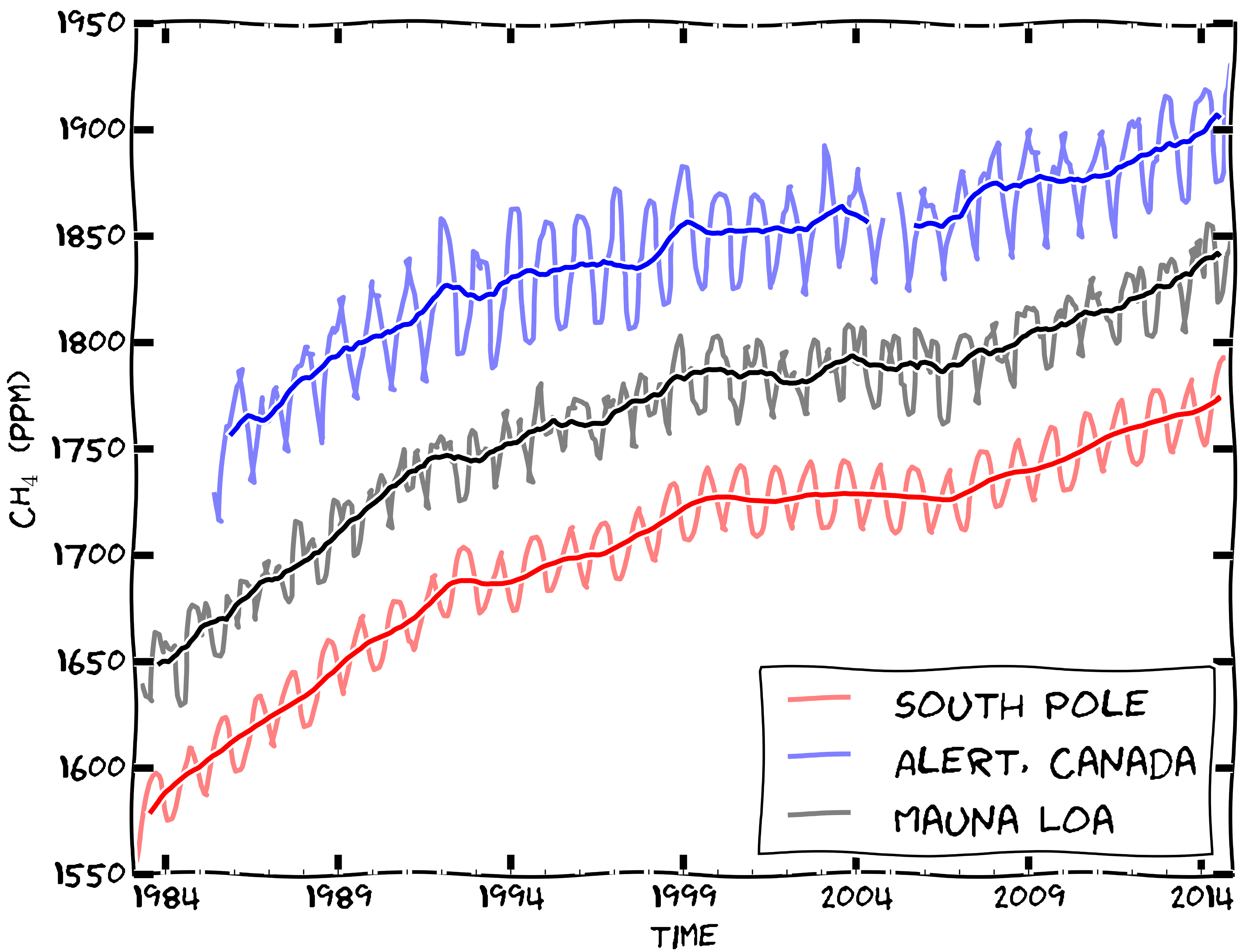

Recent changes in atmospheric methane

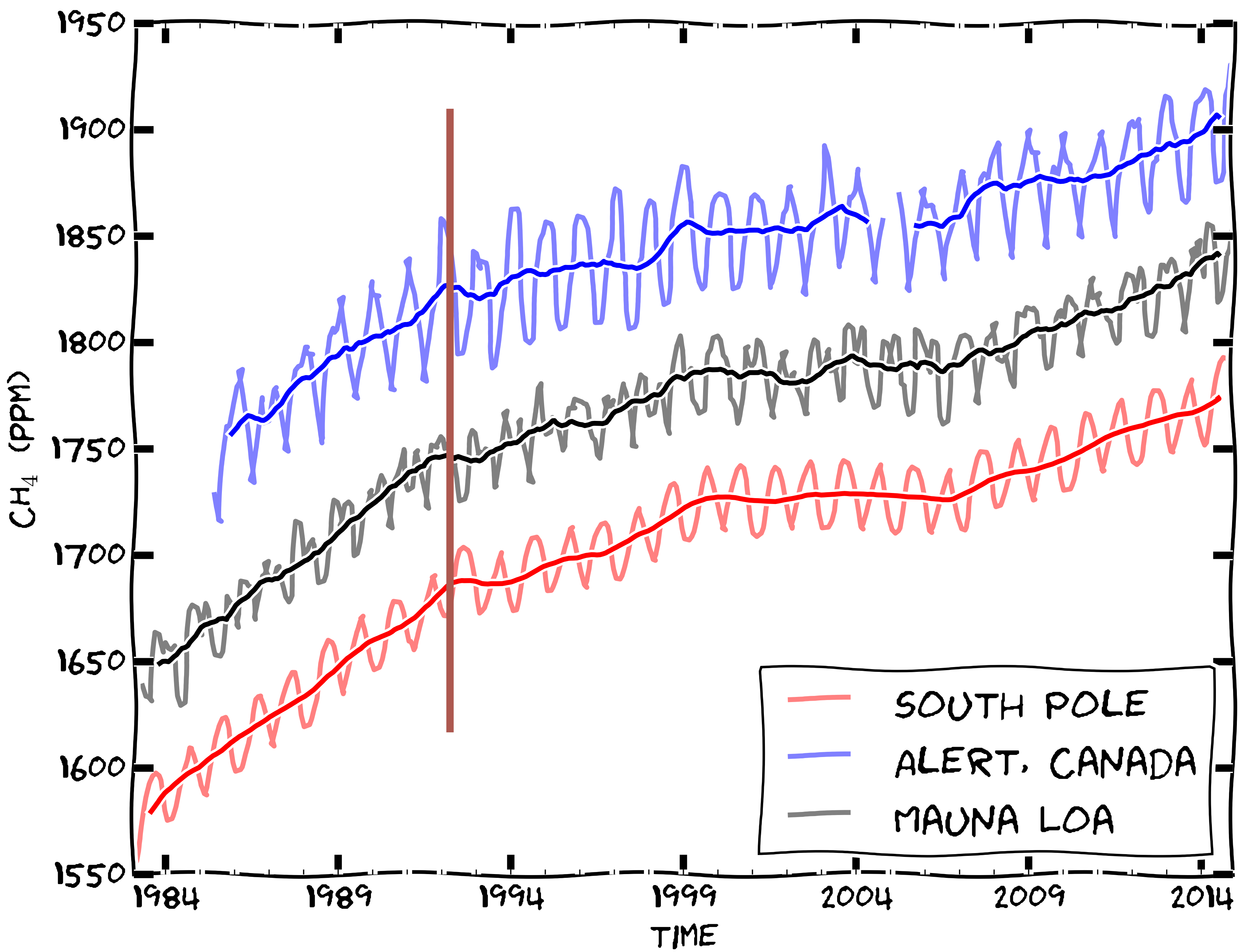

Recent changes in atmospheric methane

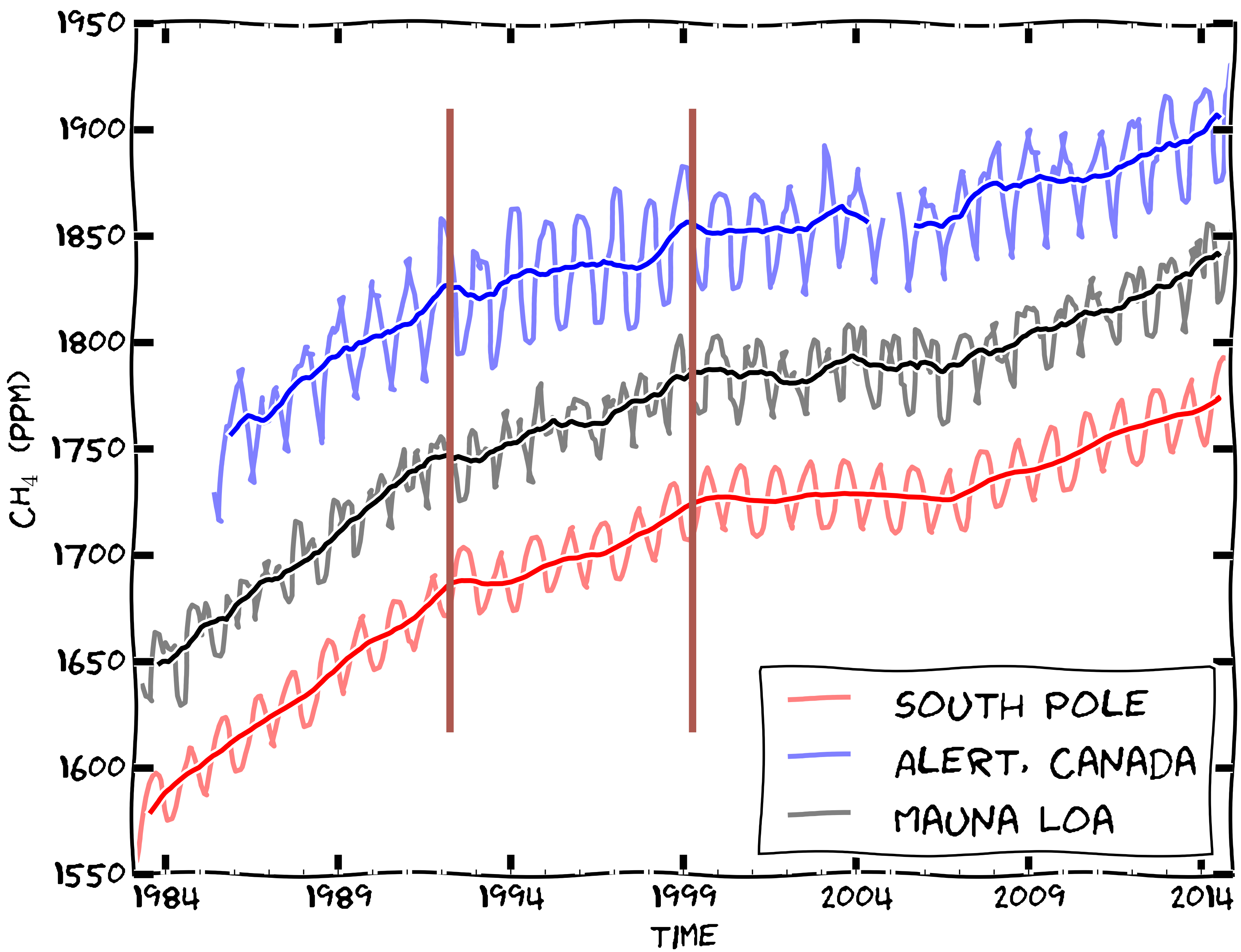

Recent changes in atmospheric methane

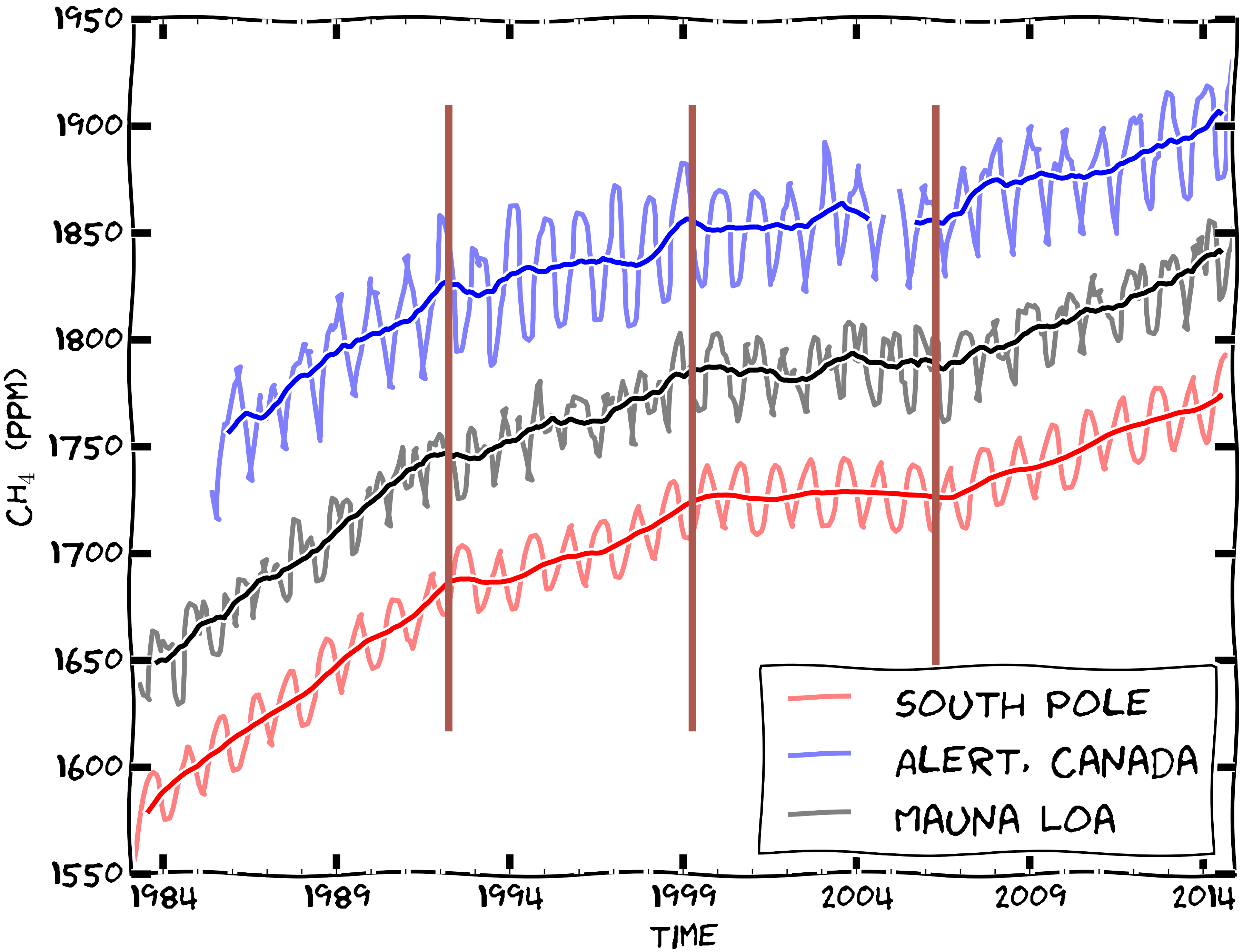

Recent changes in atmospheric methane

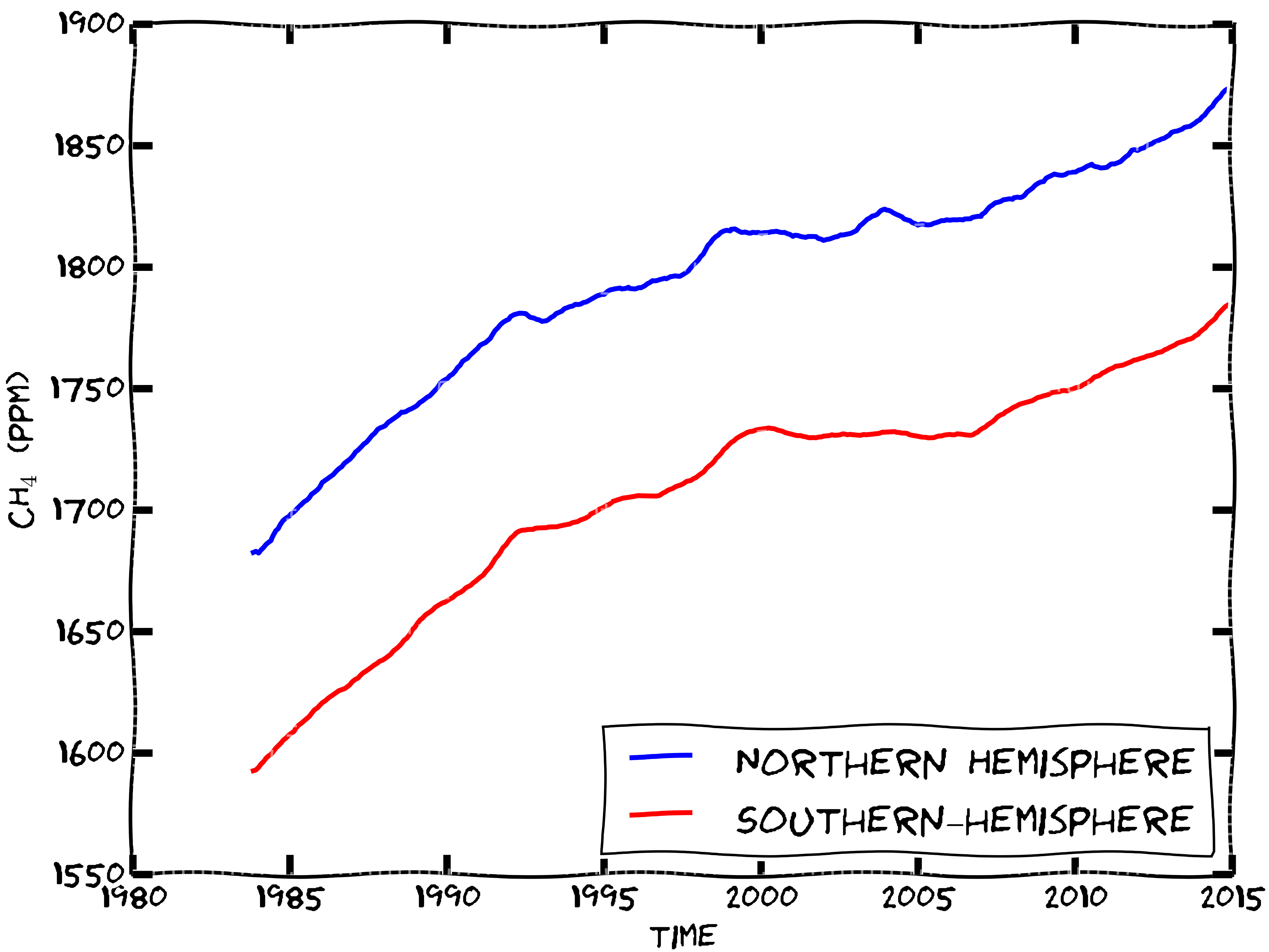

Recent changes in atmospheric methane

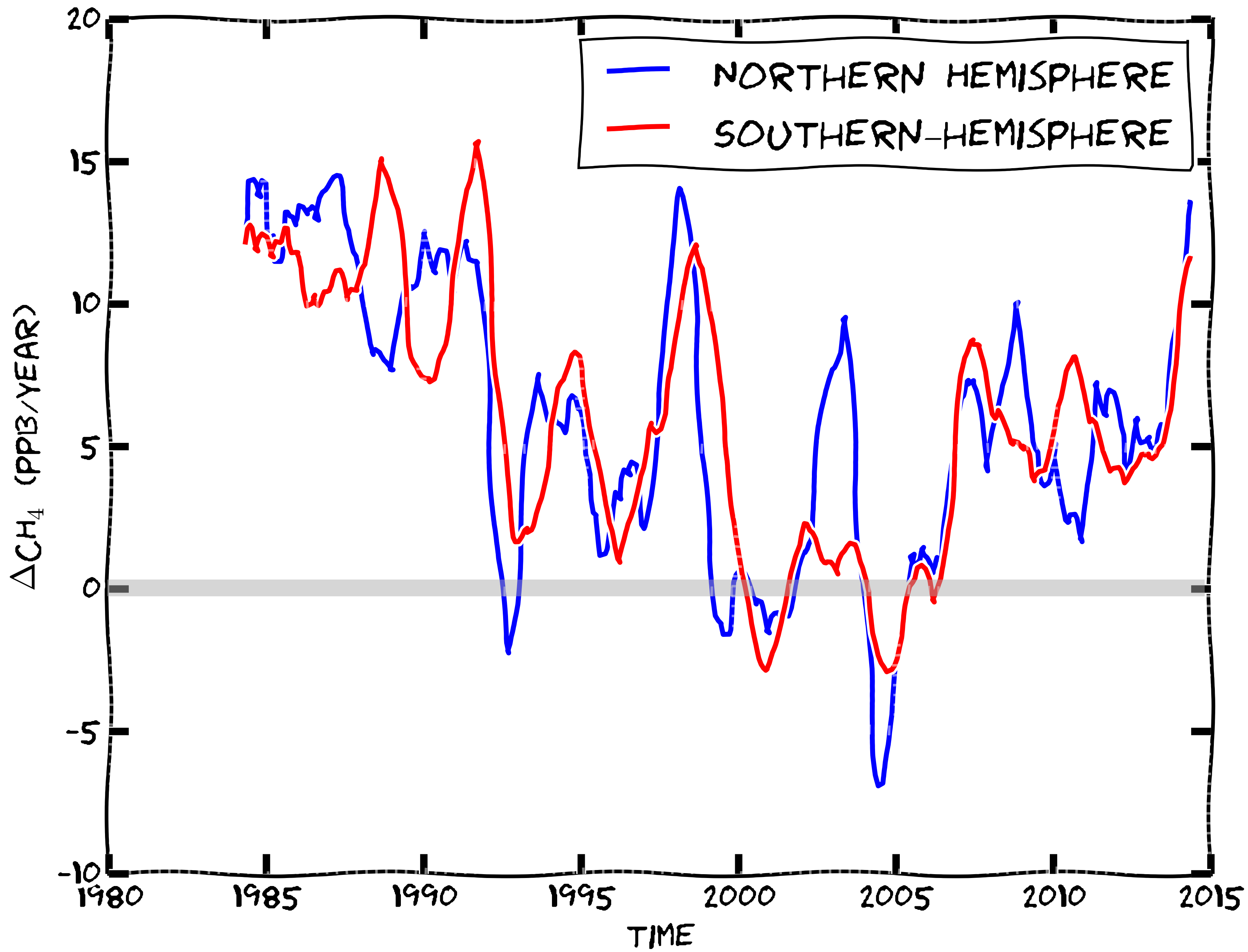

Recent changes in atmospheric methane

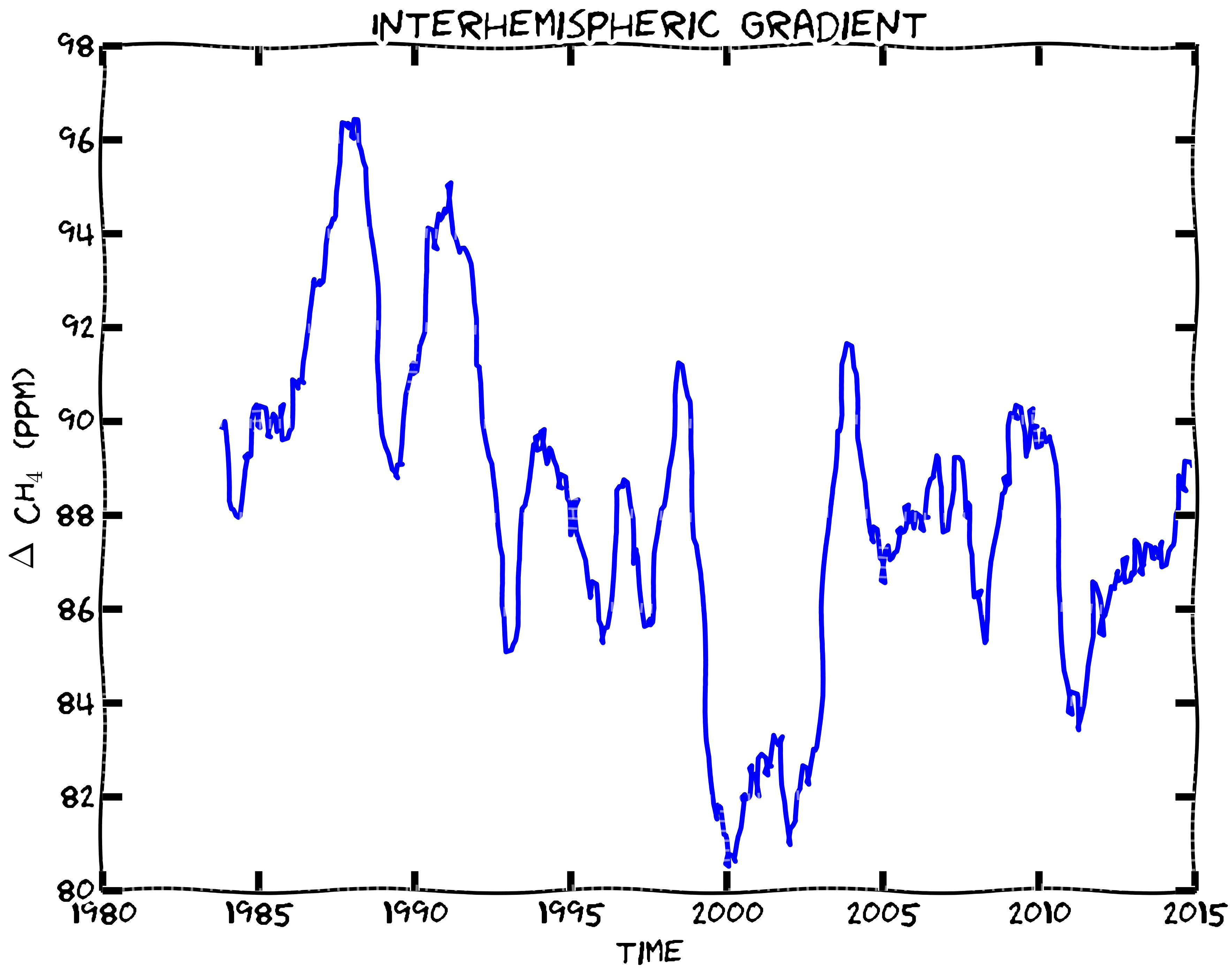

Recent changes in atmospheric methane

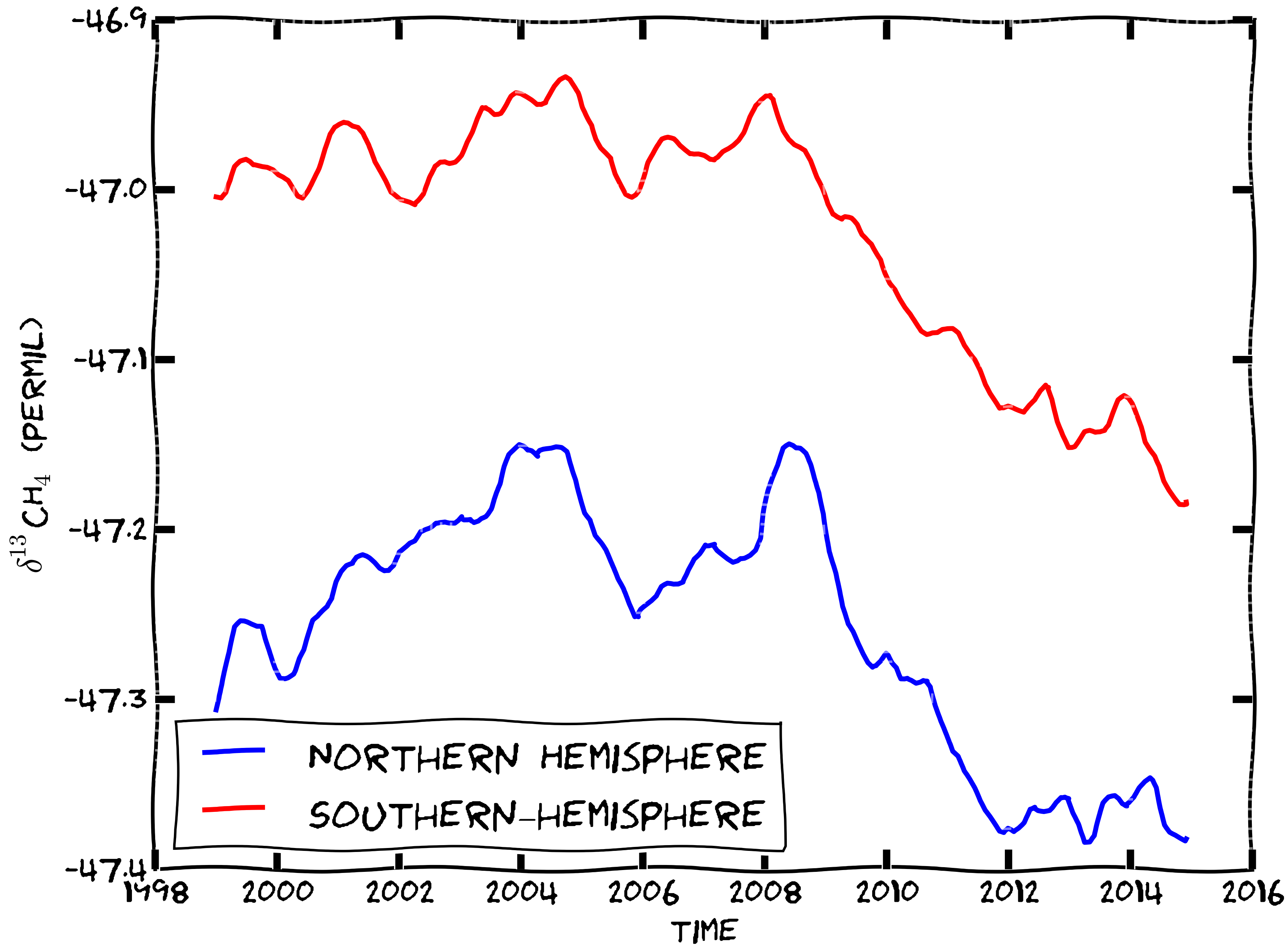

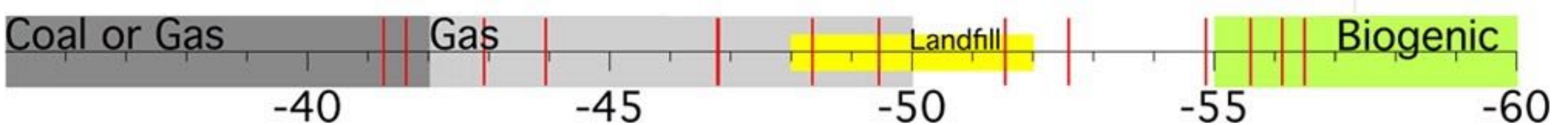

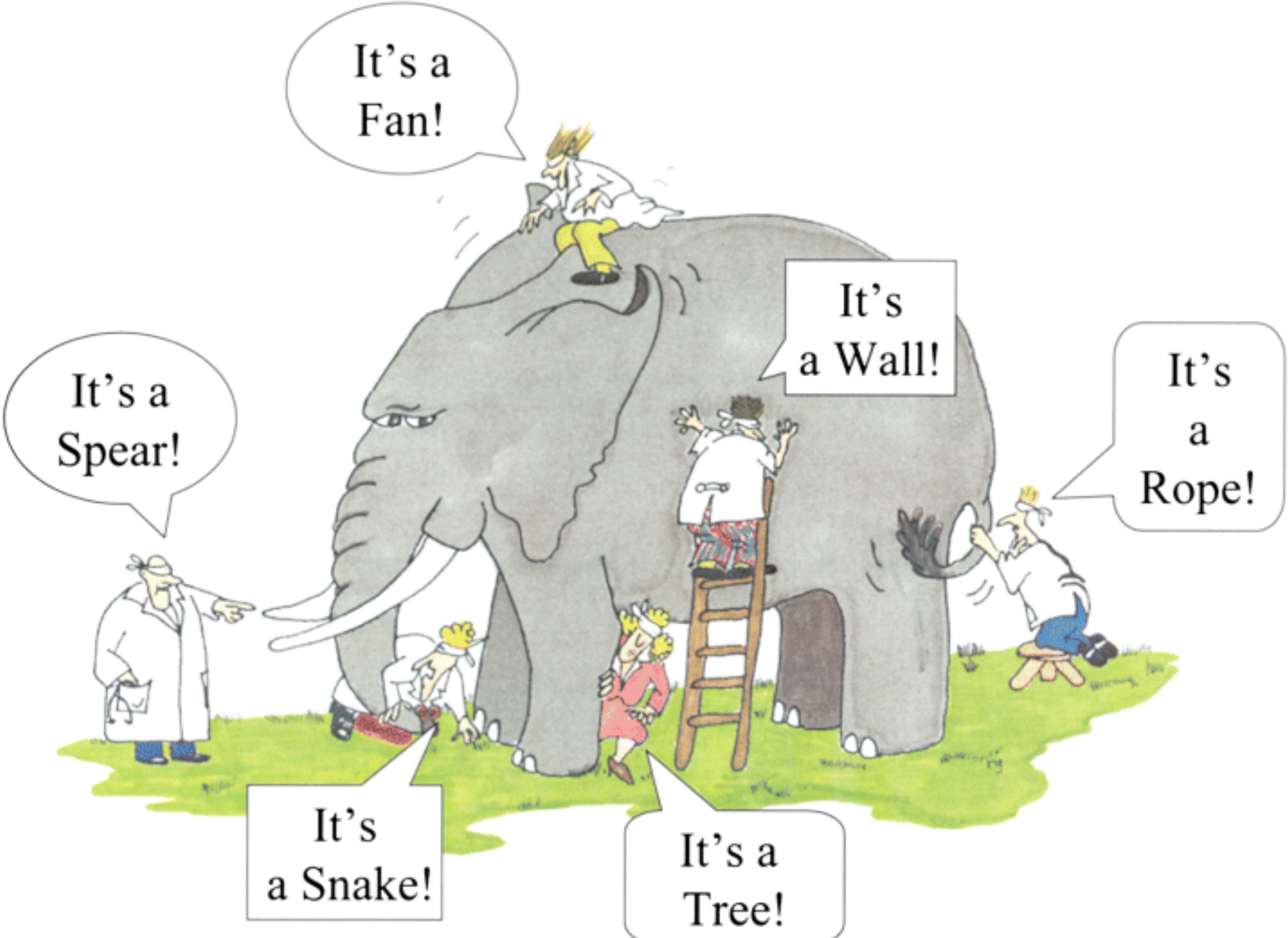
It's a Spear!
It's a Fan!
It's a Snake!
It's a Tree!
It's a Wall!
It's a Rope!

Another look at it

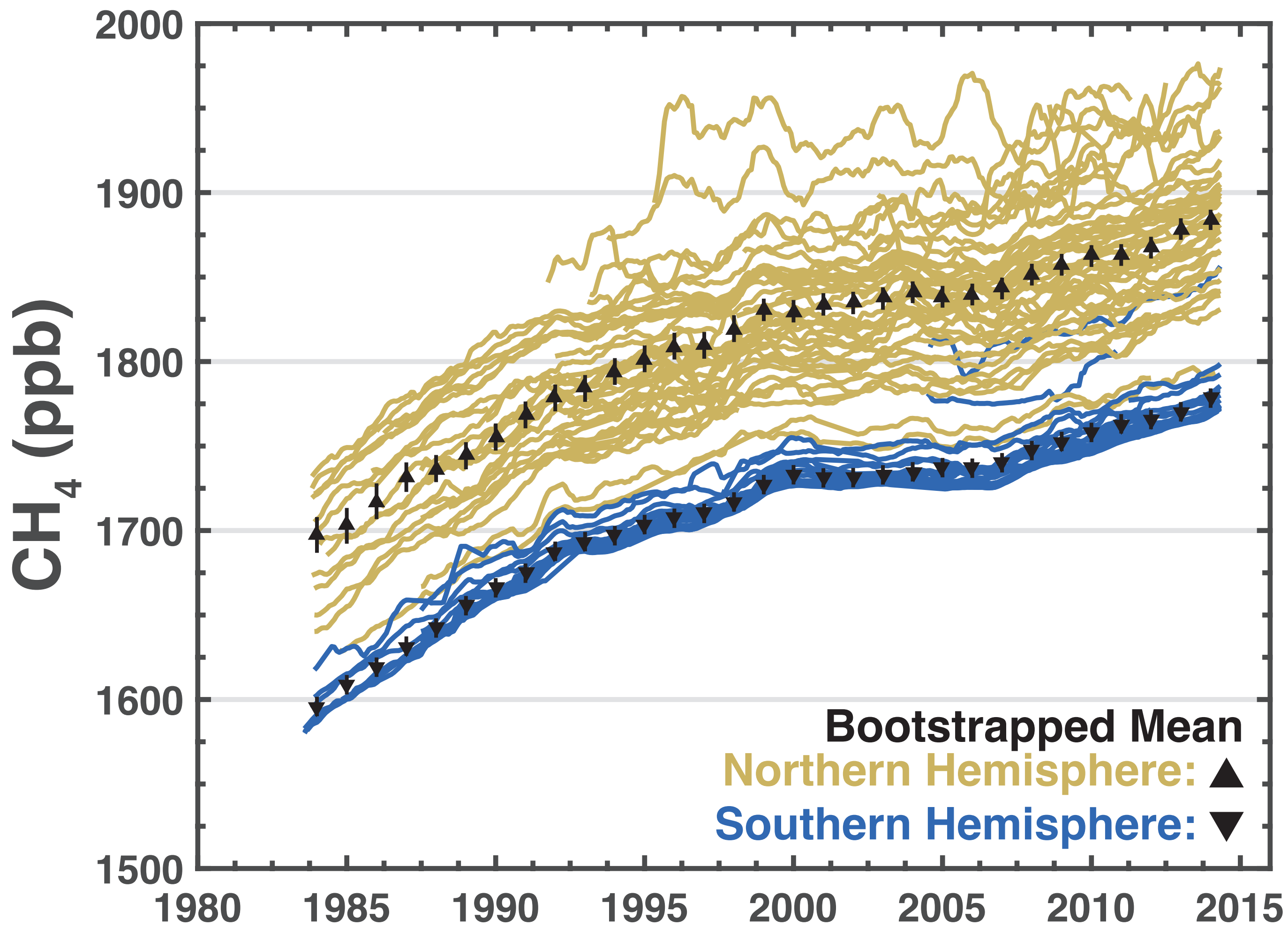

- De-seasonalize observational records from each site
- Split observations based on hemisphere
- Bootstrap hemispheric averages and uncertainties

Data from NOAA/ESRL[1,2,3], U. Heidelberg[2], UCI[2], UW[2], & GAGE/AGAGE 1 = CH_4, 2 = $\delta^{13}CH_4$, 3 = CH_3CCl_3

Methylchloroform

- Used as solvent and insecticide prior to the Montreal Protocol (is also ozone depleting substance)
- Emissions phased out in 1989

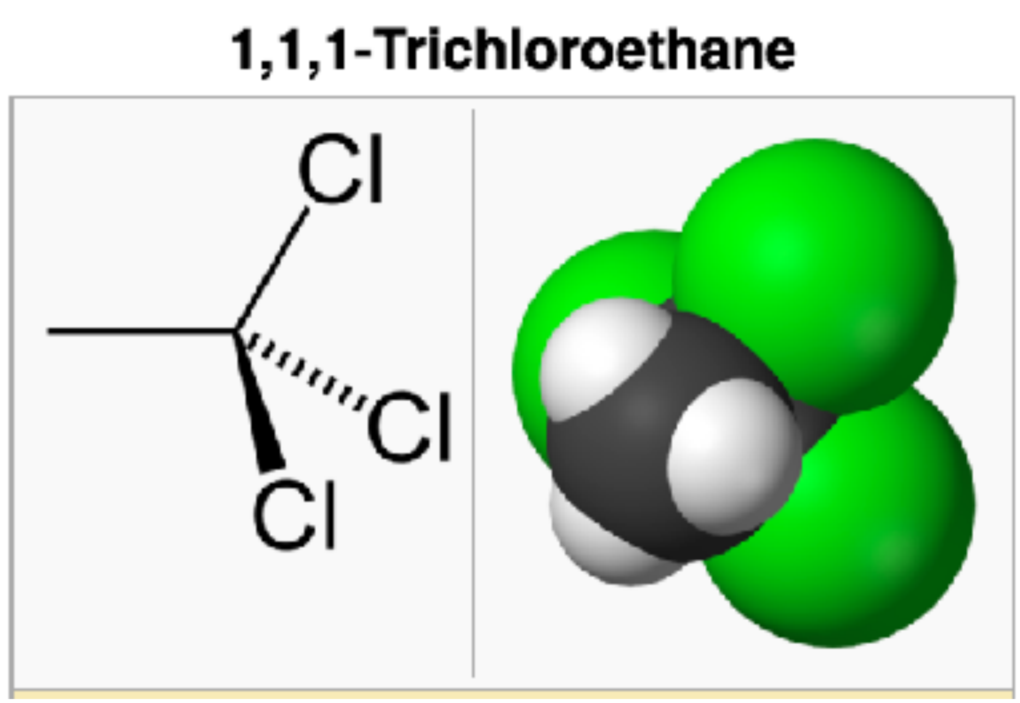

Ambiguity in the causes for decadal trends in atmospheric methane and hydroxyl

Turner, Frankenberg, Wennberg, Jacob (in press, PNAS)

Can use a simple 2-box model:

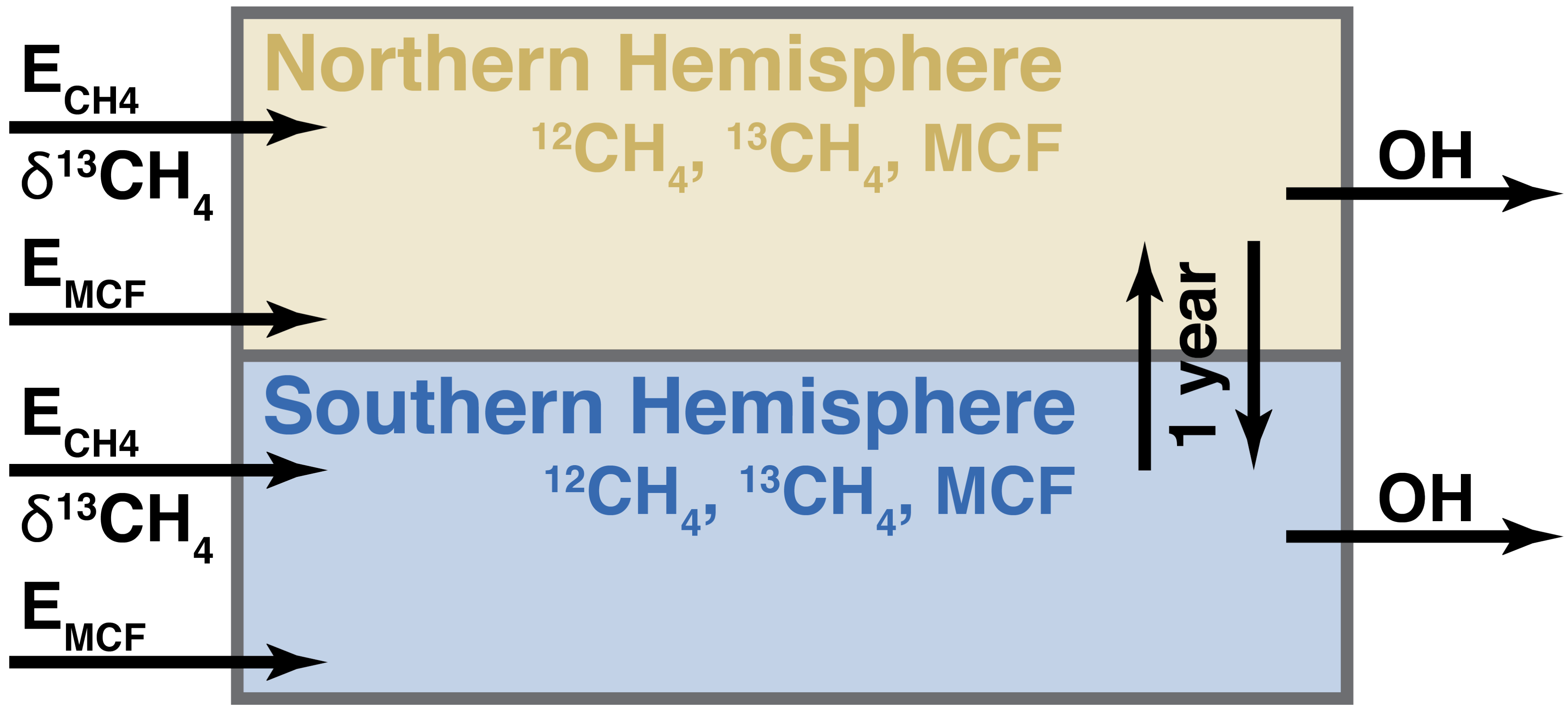

$$\frac{\partial [X]_N(t)}{\partial t} = E_{X,N}(t) - k_{[X]}[\mathrm{OH}]_N(t)[X]_N(t) + \frac{[X]_S(t) - [X]_N(t)}{\tau_{\mathrm{NS}}}$$

$$\frac{\partial [X]_S(t)}{\partial t} = E_{X,S}(t) - k_{[X]}[\mathrm{OH}]_S(t)[X]_S(t) + \frac{[X]_N(t) - [X]_S(t)}{\tau_{\mathrm{NS}}}$$

Jacobians

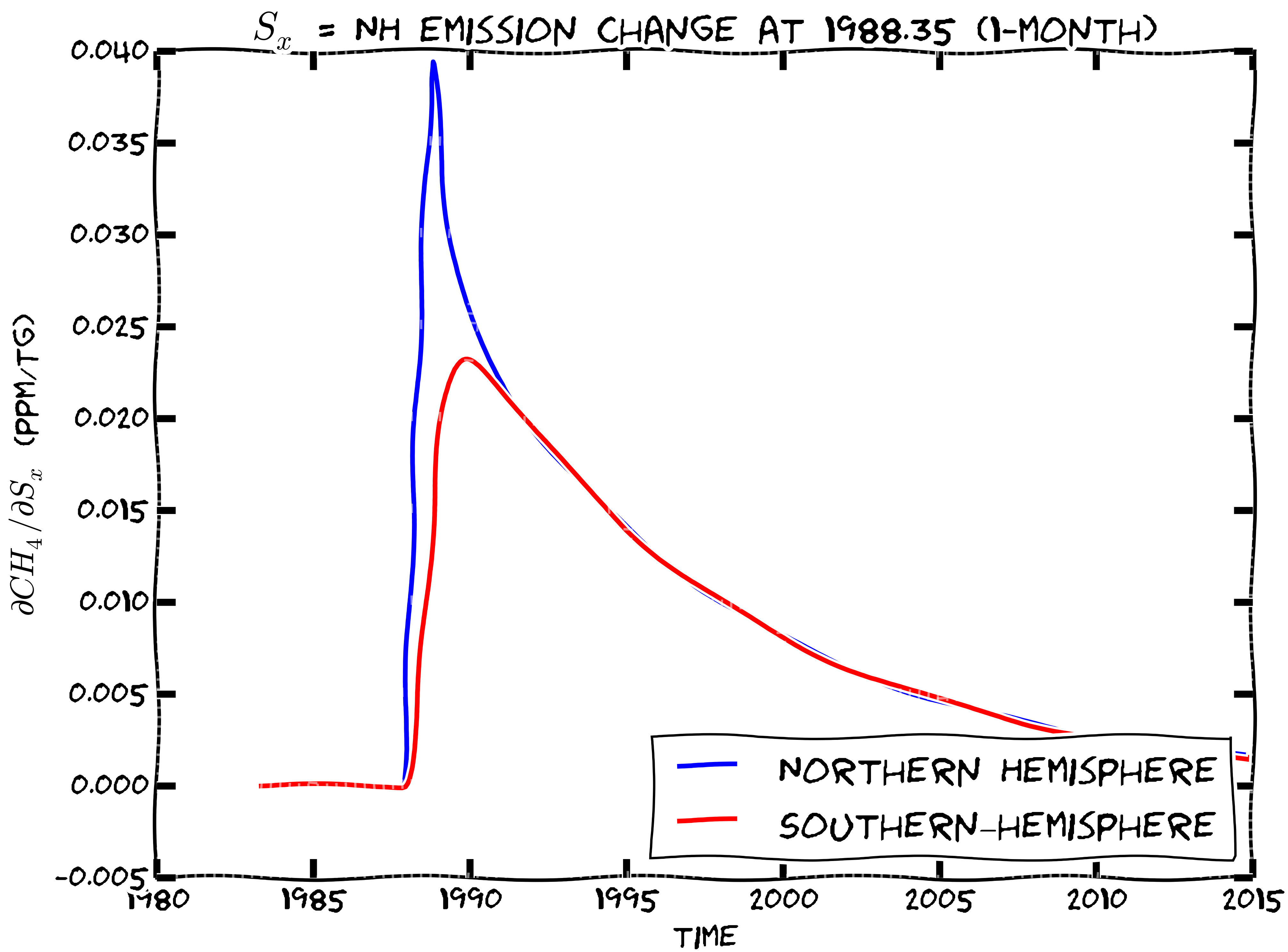

S_x = NH EMISSION CHANGE AT 1988.35 (1-MONTH)
0.040
0.035
0.030
0.025
0.020
0.015
0.010
0.005
0.000
-0.005
$\partial CH_4 / \partial S_x$ (PPM/TG)
1980
1985
1990
1995
2000
2005
2010
2015
TIME
NORTHERN HEMISPHERE
SOUTHERN-HEMISPHERE

Jacobians

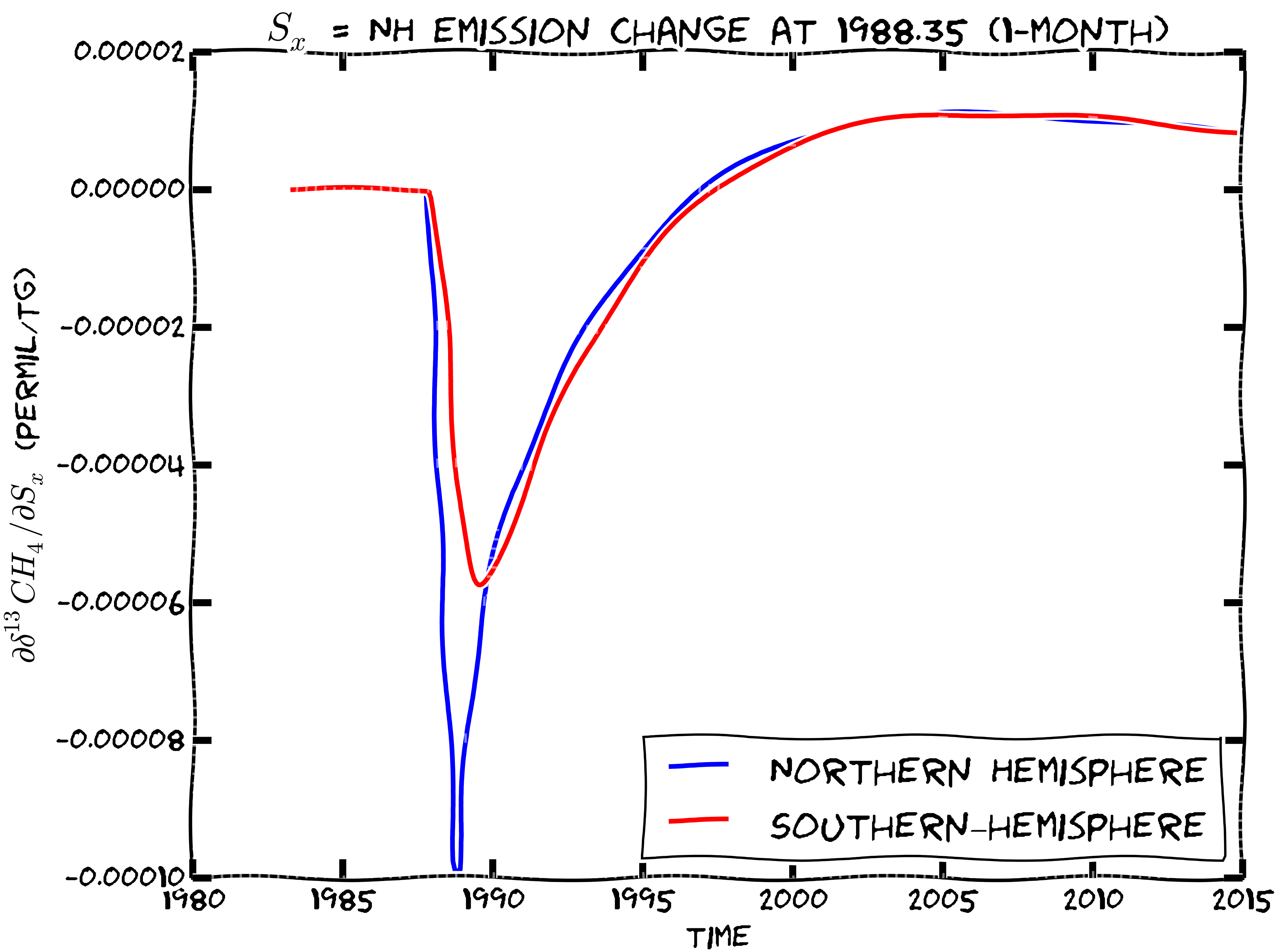

S_x = NH EMISSION CHANGE AT 1988.35 (1-MONTH)
0.00002
0.00000
-0.00002
-0.00004
-0.00006
-0.00008
-0.00010
$\partial\delta^{13}CH_4/\partial S_x$ (PERMIL/TG)
1980
1985
1990
1995
2000
2005
2010
2015
TIME
NORTHERN HEMISPHERE
SOUTHERN-HEMISPHERE

Jacobians

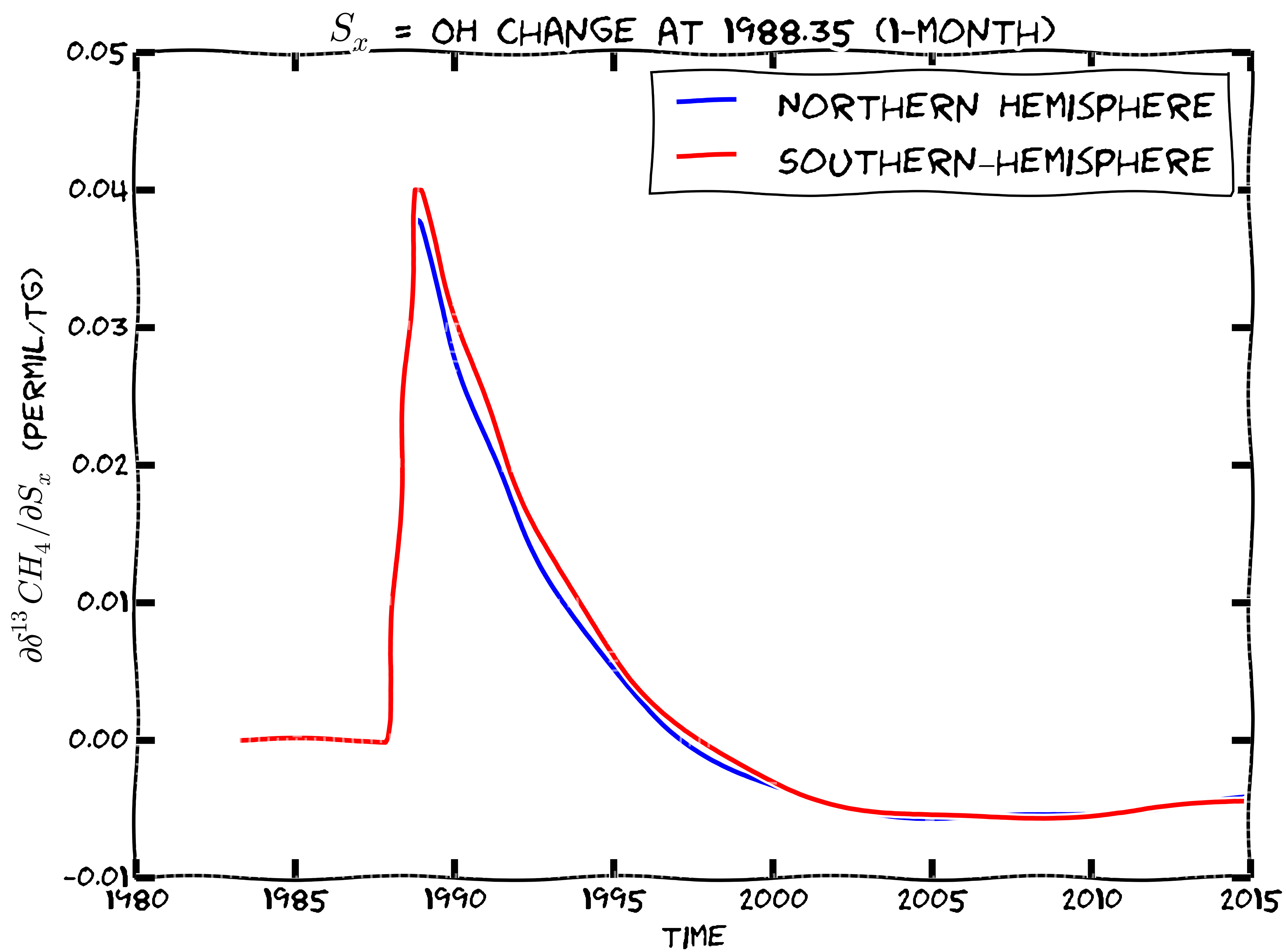

S_x = OH CHANGE AT 1988.35 (1-MONTH)
NORTHERN HEMISPHERE
SOUTHERN-HEMISPHERE
$\partial\delta^{13}CH_4/\partial S_x$ (PERMIL/TG)
0.05
0.04
0.03
0.02
0.01
0.00
-0.01
1980
1985
1990
1995
2000
2005
2010
2015
TIME

Fits

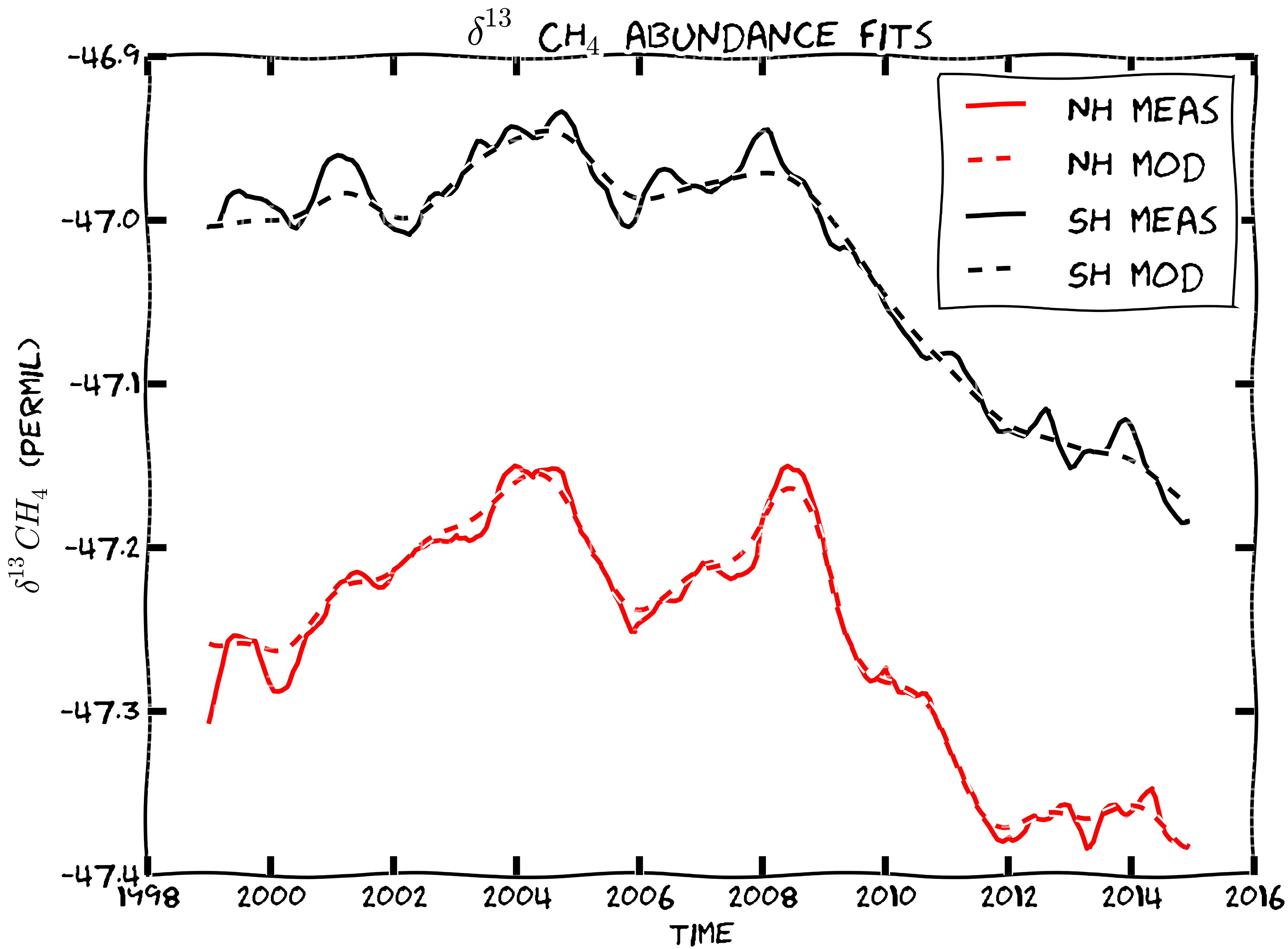

δ^{13} CH$_4$ ABUNDANCE FITS
-46.9
-47.0
-47.1
-47.2
-47.3
-47.4
$\delta^{13}CH_4$ (PERMIL)
1998
2000
2002
2004
2006
2008
2010
2012
2014
2016
TIME
NH MEAS
NH MOD
SH MEAS
SH MOD

Formal Inversion

- Minimize

$$(\mathbf{x}-\mathbf{x_a})^T \mathbf{S_a}^{-1}(\mathbf{x}-\mathbf{x_a}) + (\mathbf{y}-\mathbf{Kx})^T \mathbf{S}_{\varepsilon}^{-1}(\mathbf{y}-\mathbf{Kx})$$

State vector x (size 2940) includes:
NH and SH emissions each month
isotopic composition of those
OH scaling factor for each month

Measurement vector y (size 2280) size includes:
NH and SH abundances
NH and SH isotopic composition
NH and SH MCF abundances

Prior run

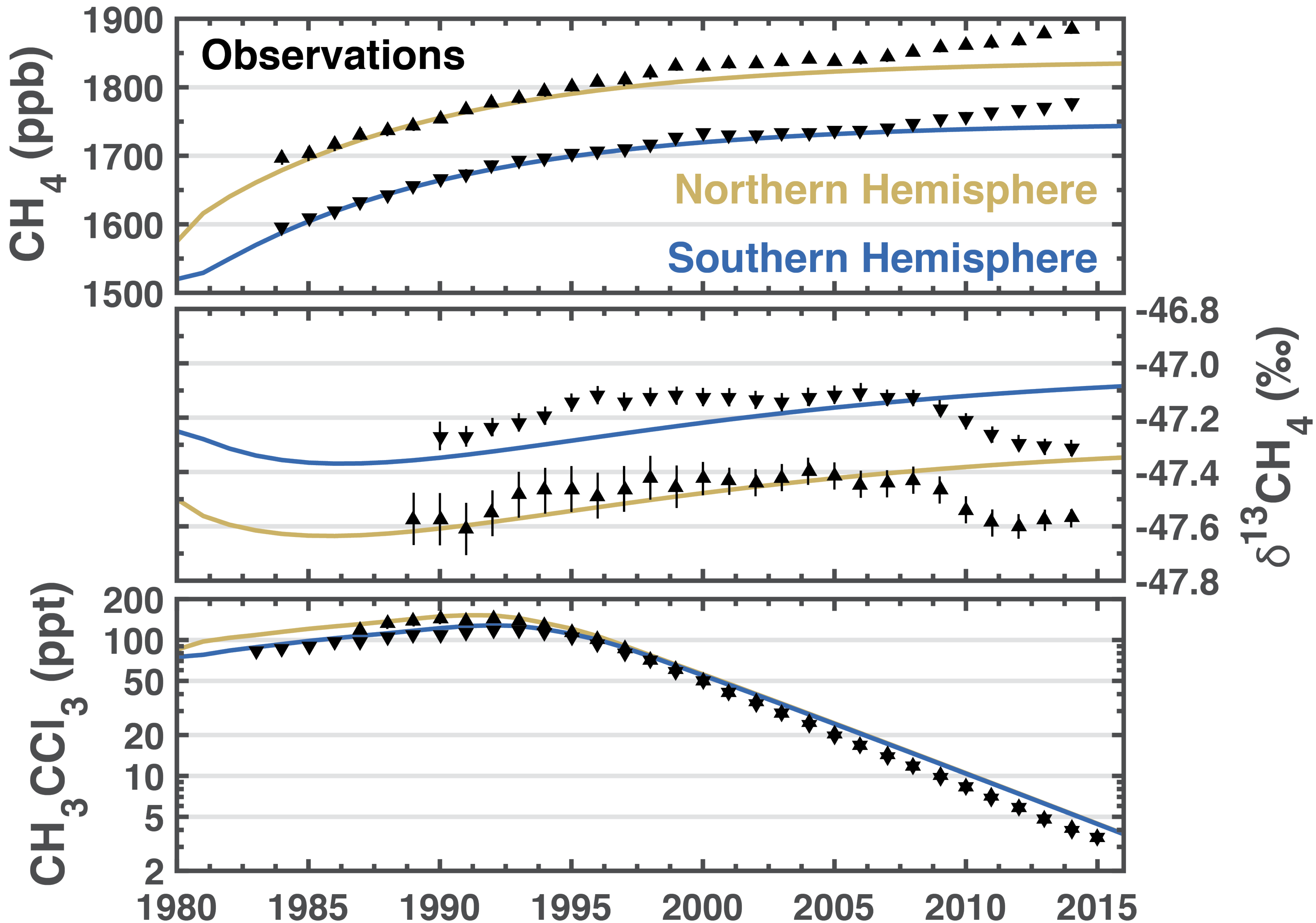

Observations
Northern Hemisphere
Southern Hemisphere
CH4 (ppb)
1900
1800
1700
1600
1500
δ13CH4 (‰)
-46.8
-47.0
-47.2
-47.4
-47.6
-47.8
CH3CCl3 (ppt)
200
100
50
20
10
5
2
1980
1985
1990
1995
2000
2005
2010
2015

Posterior (non-linear inversion)

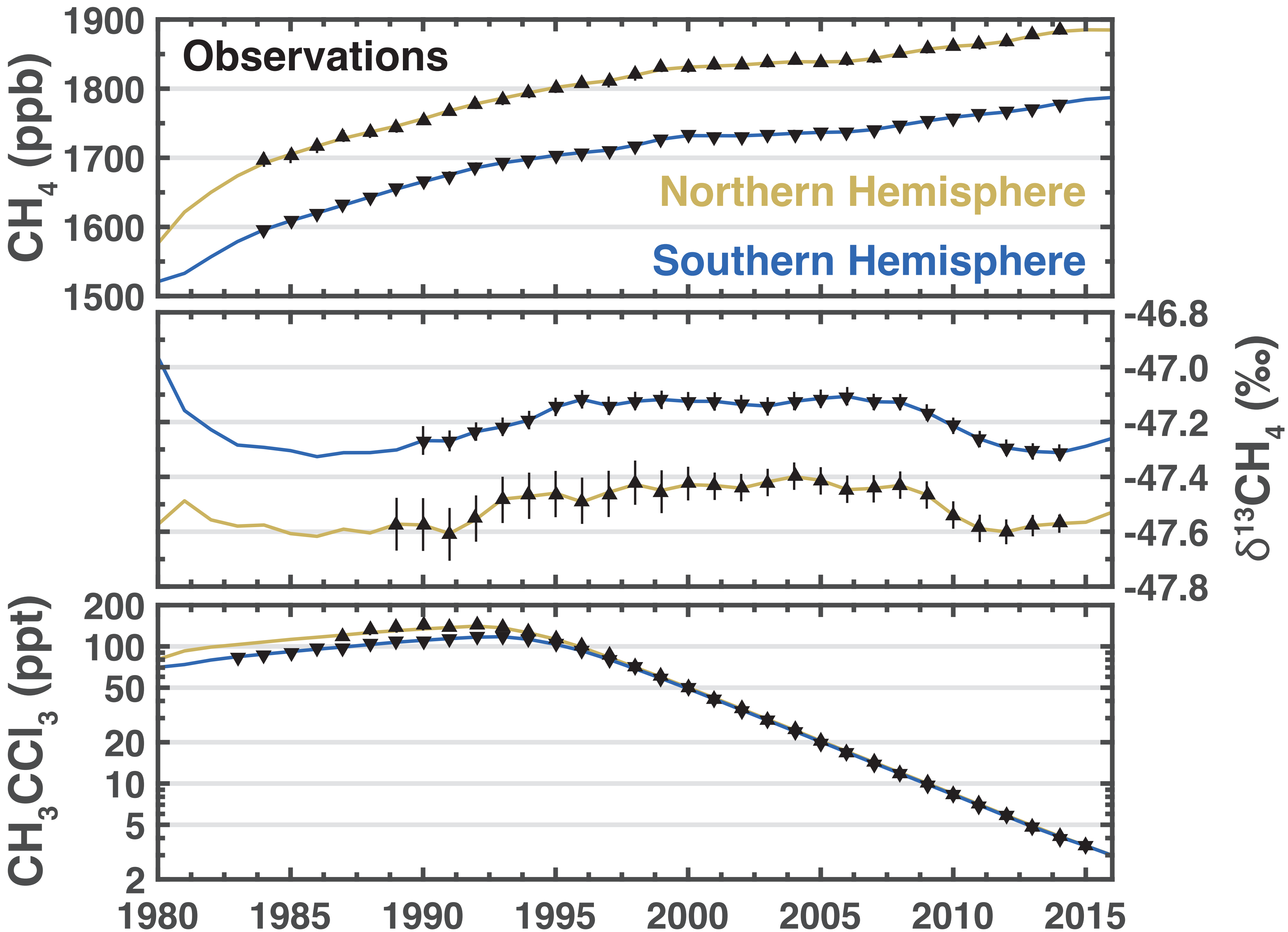

Flux Inversion — CH_4 lifetime fixed

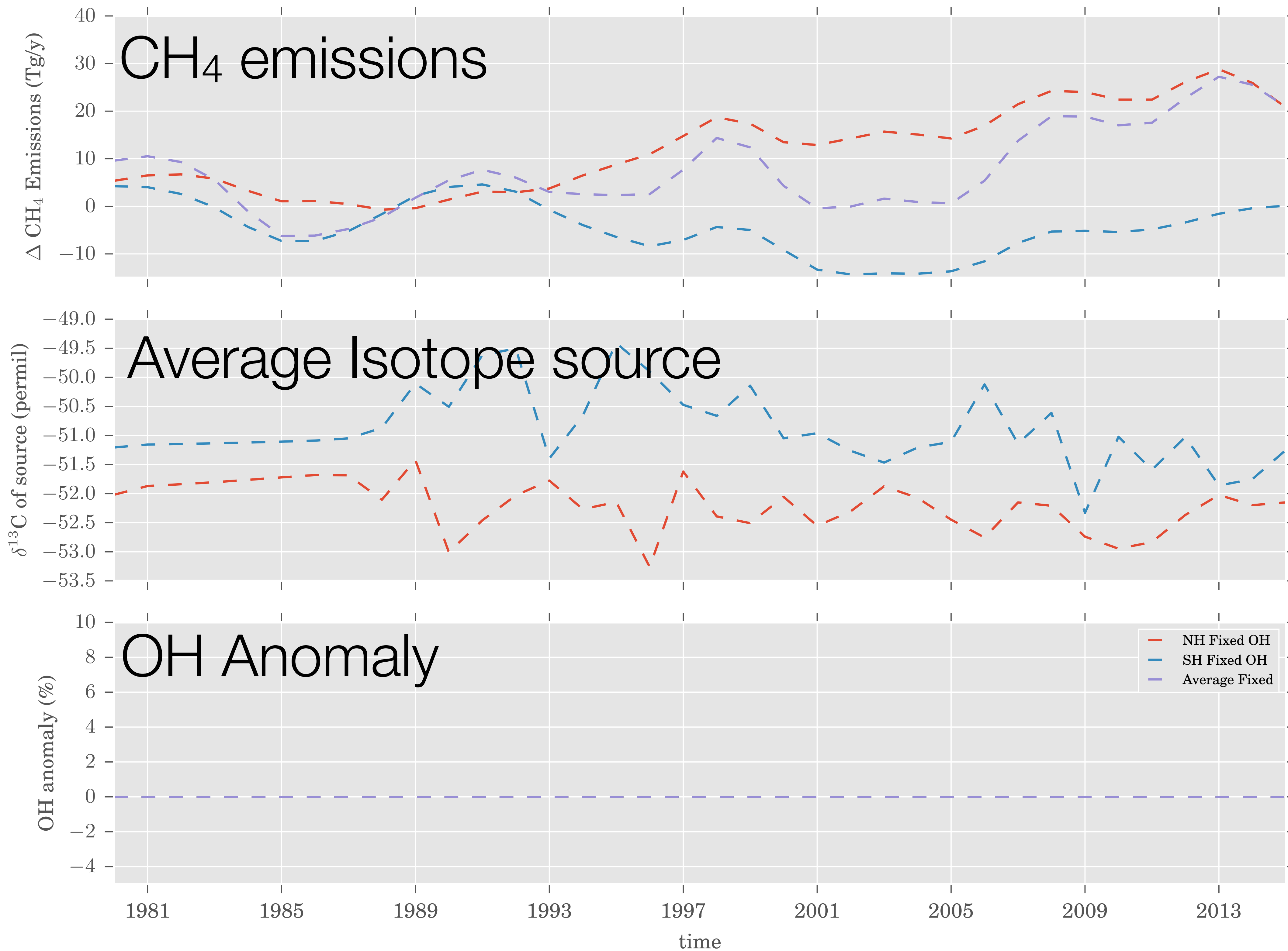

With OH fitted (through MCF measurements)

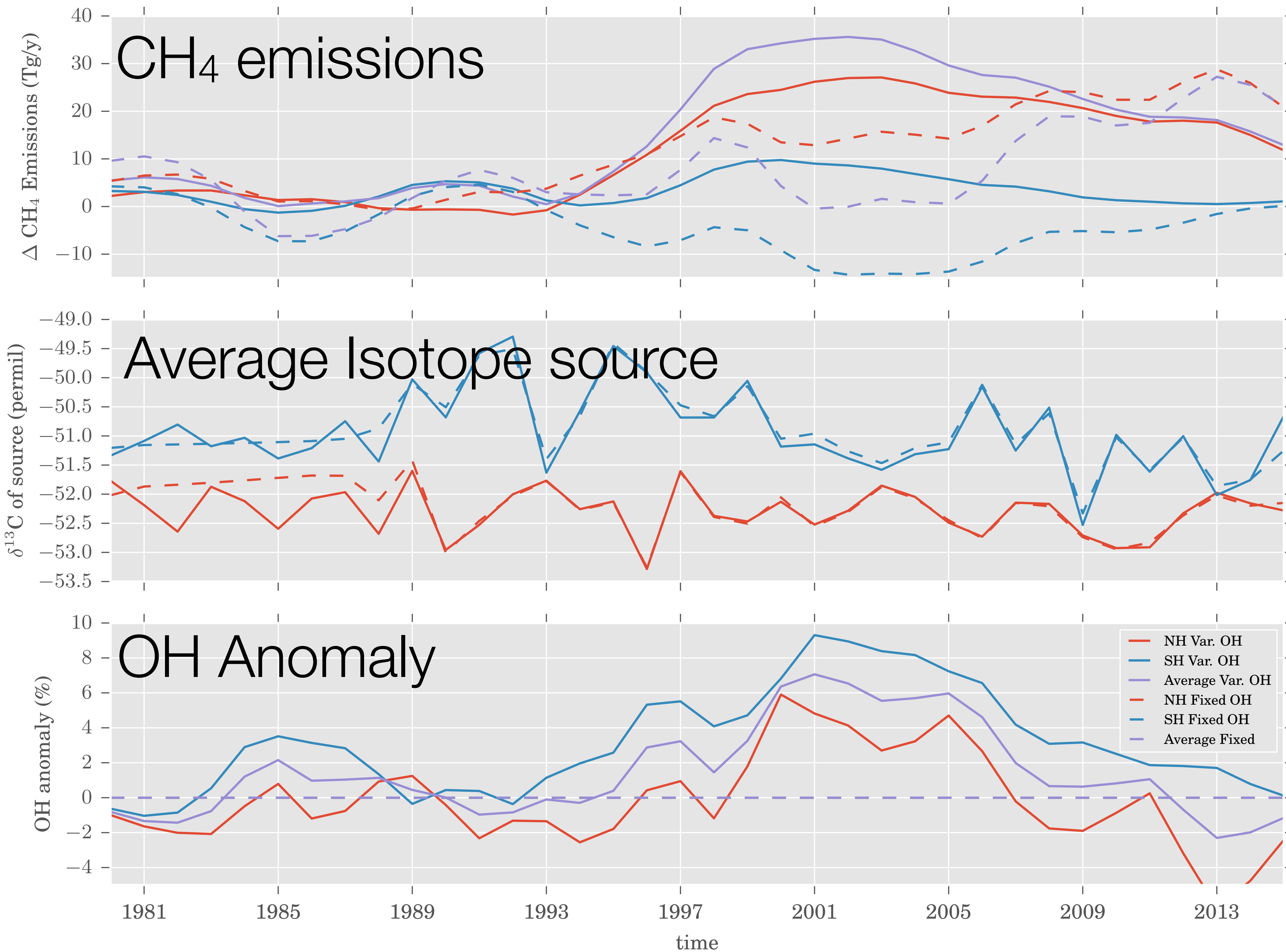

With OH fitted (through MCF measurements)

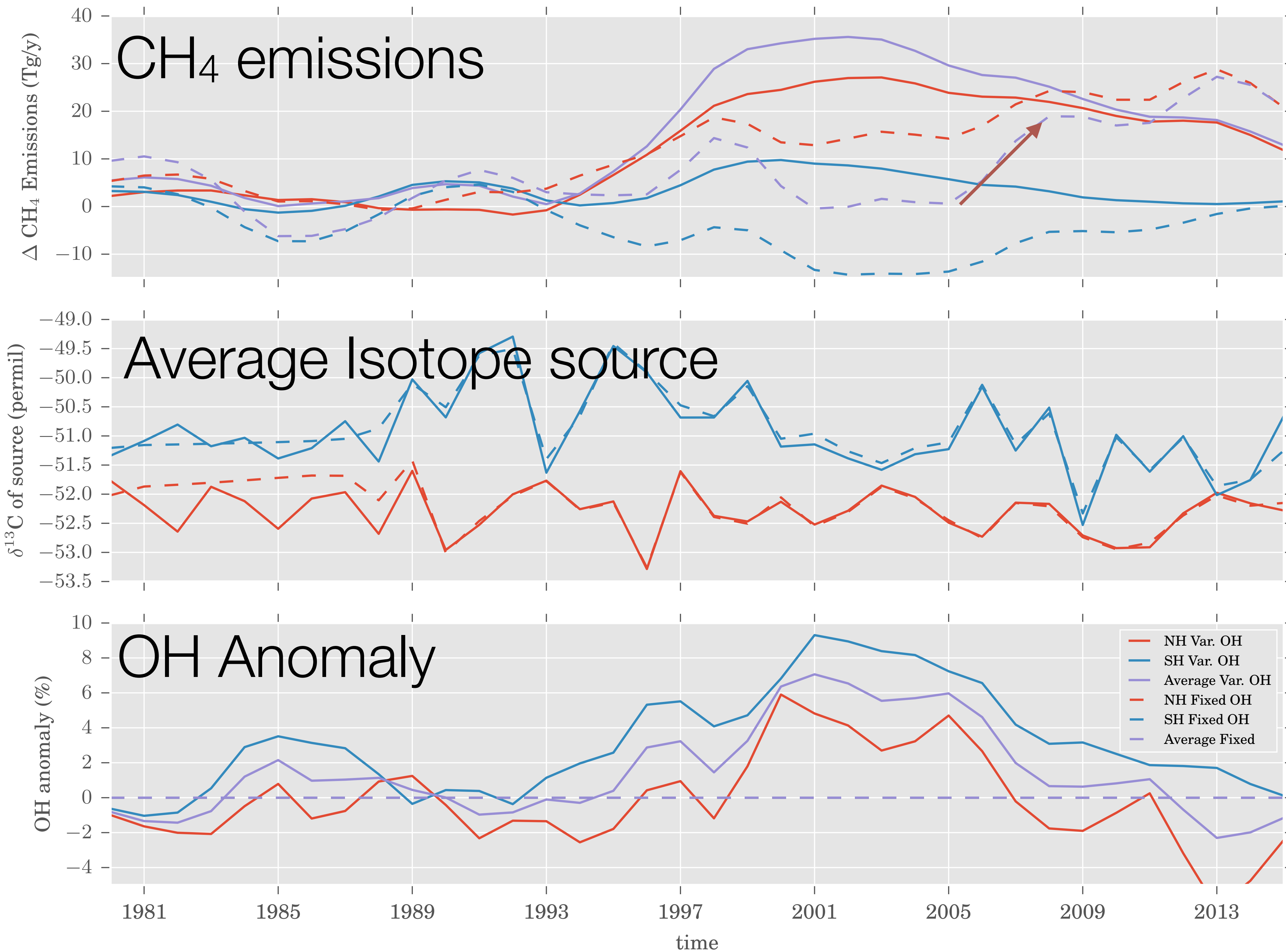

With OH fitted (through MCF measurements)

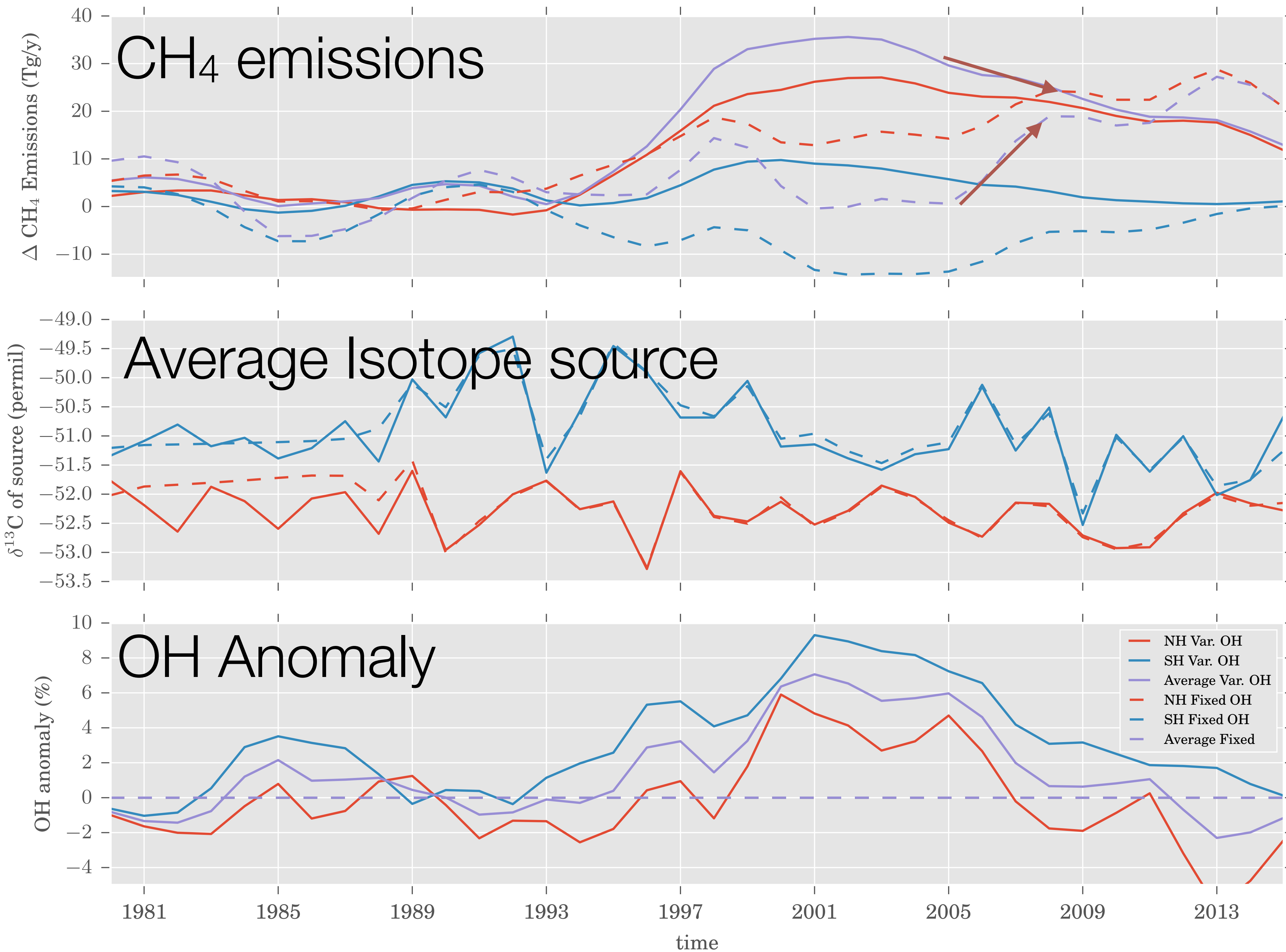

Is OH variation realistic?

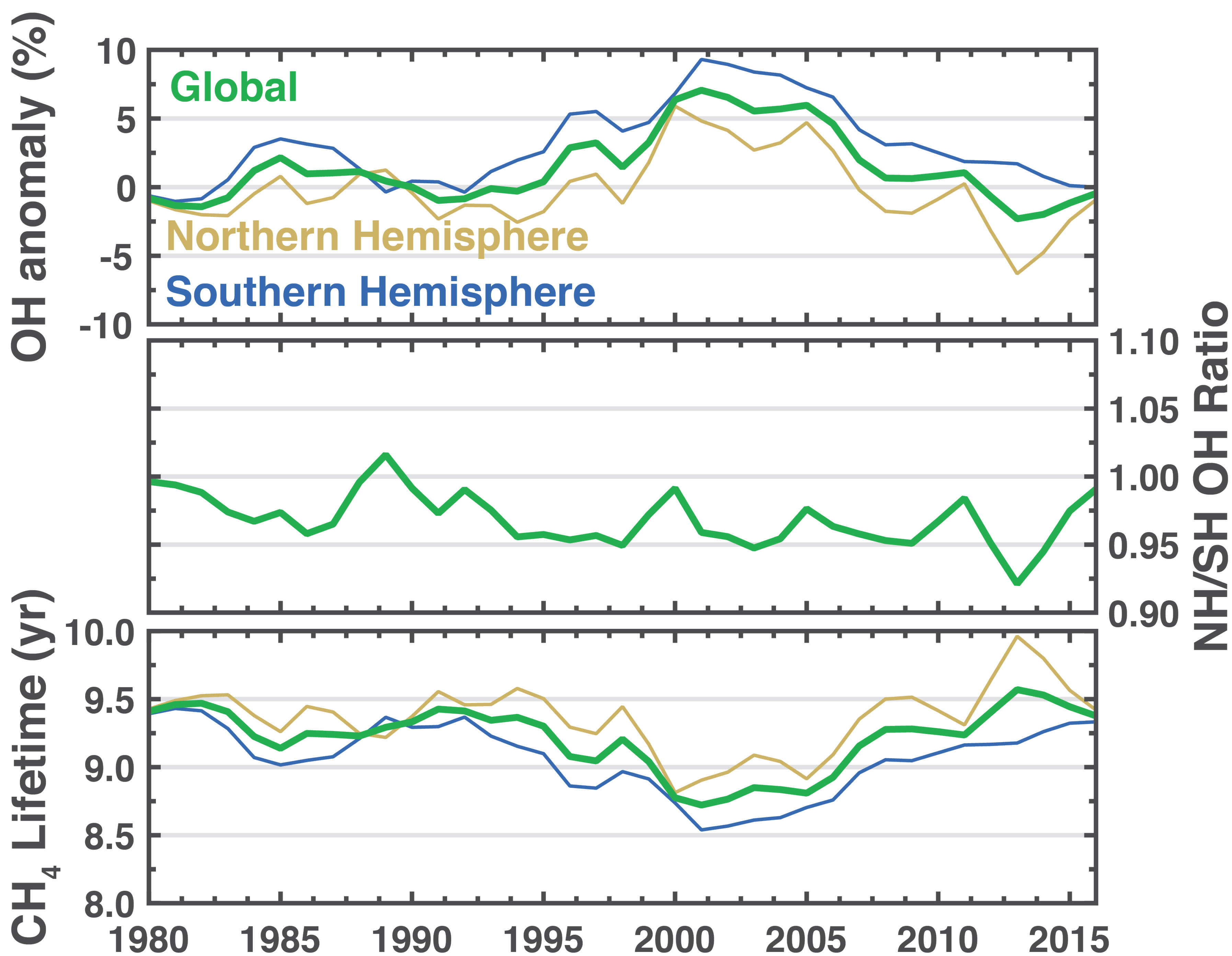

Previous publications find a similar behavior

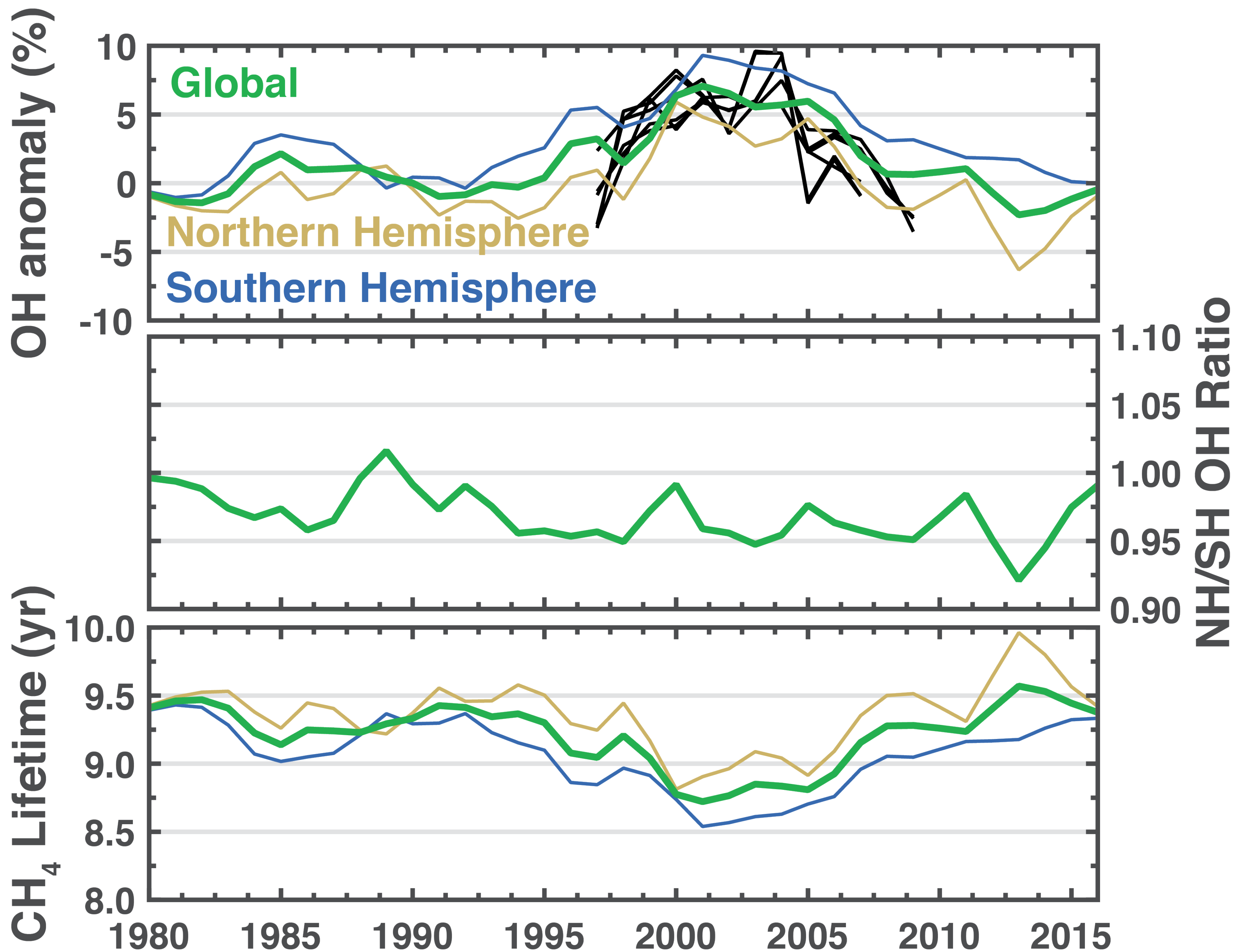

Montzka *et al.*, Rigby *et al.*, & McNorton *et al.* find similar OH anomalies

Holmes et al

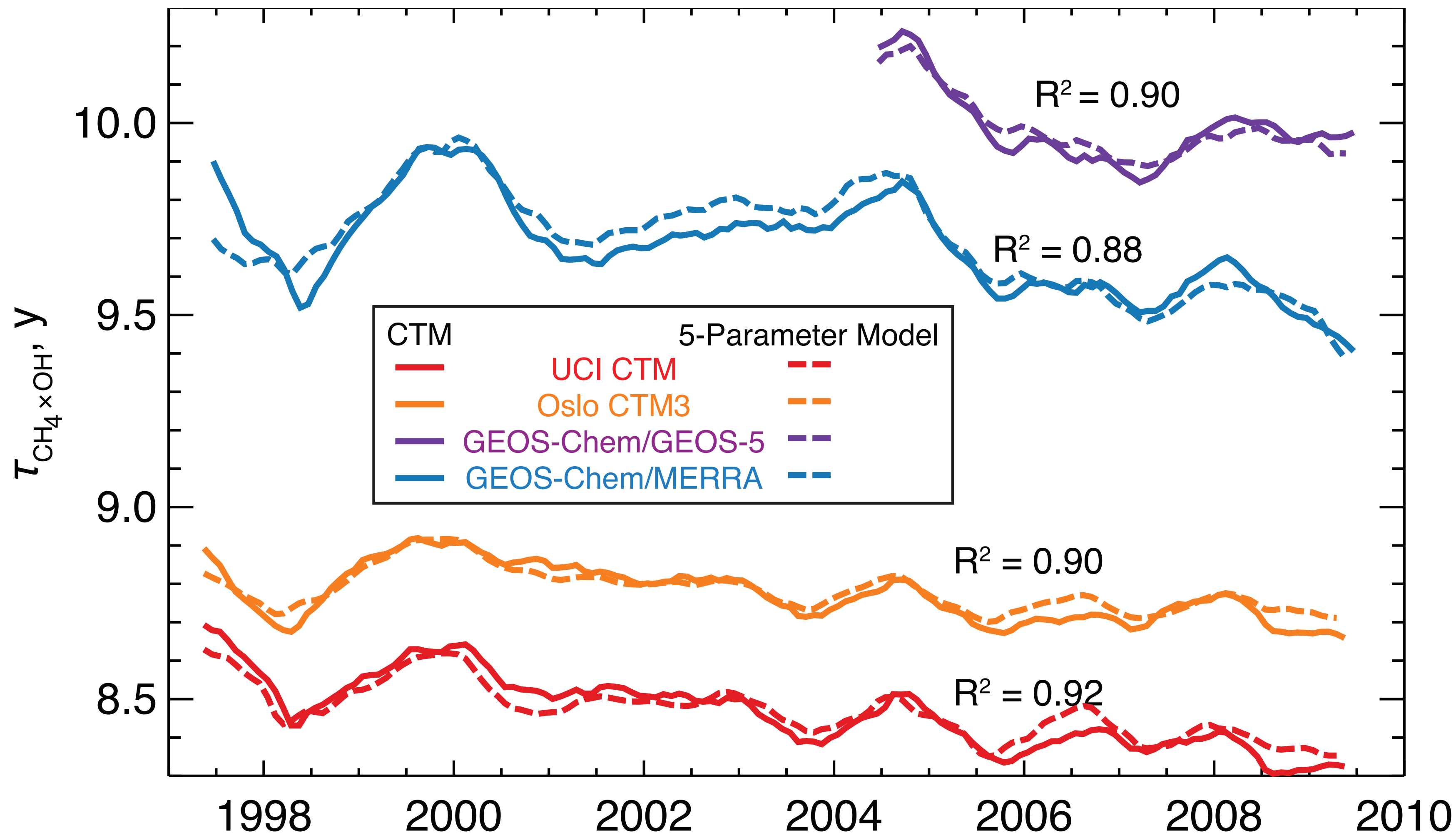

Fig. 1. Methane lifetime due to oxidation by tropospheric OH ($\tau_{CH_4 \times OH}$) simulated by each CTM (solid lines) and reconstructed from the 5-parameter model (dashed lines). The parameters are air temperature, water vapor, ozone column, lightning NO_x emission, and biomass burning emission. Parameter values for each CTM are

Mode times — Prather

Assume that V is a solution for a generic operator A, $\mathrm{d}V/\mathrm{d}t = A[V]$, then the continuity equation for a perturbation δV can be derived as

$$\frac{\mathrm{d}\delta V}{\mathrm{d}t} = \frac{\mathrm{d}[V + \mathrm{d}V]}{\mathrm{d}t} - \frac{\mathrm{d}V}{\mathrm{d}t} = A[V + \delta V] - A[V] = J_V \cdot \delta V + \mathrm{order}(\delta V^2),$$

where the Jacobian matrix J of the operator A is the first term in the Taylor expansion of $A[V+\delta V]$ evaluated at V, i.e. the linearized system (e.g. Prather 1996, 2002; Manning 1999). The Jacobian matrix has dimension $m \times m$, where m is the number of variables. Species are inherently discrete, and adopting a discrete spatial grid gives us a finite number of variables across (x, y, z, n). For discussion of the continuum, see §8.

If the perturbation δV is an eigenvector of J_V with eigenvalue λ, then

$$\frac{\mathrm{d}\delta V}{\mathrm{d}t} = J_V \cdot \delta V = \lambda \delta V,$$

Coupled OH Chemistry — Prather

Consider a simplified model of the CH_4–CO–OH chemical system as having three reactions

(i) $CH_4 + OH \Rightarrow \cdots \Rightarrow CO$ $\quad R_5 = k_5[CH_4][OH]$ $\quad k_5 = 1.266 \times 10^{-7}\ s^{-1}\ ppt^{-1}$

(ii) $CO + OH \Rightarrow \cdots$ $\quad R_6 = k_6[CO][OH]$ $\quad k_6 = 5.08 \times 10^{-6}\ s^{-1}\ ppt^{-1}$

(iii) $OH + X \Rightarrow \cdots$ $\quad R_7 = k_7[X][OH]$ $\quad k_7[X] = 1.062\ s^{-1}$,

$$\frac{d[CH_4]}{dt} = S_{CH_4} - R_5$$

$$\frac{d[CO]}{dt} = S_{CO} + R_5 - R_6$$

$$\frac{d[OH]}{dt} = \boxed{S_{OH}} - R_5 - R_6 - R_7.$$

$O_3 + h\nu\ (\lambda < 330\,nm) \rightarrow O(^1D) + O_2$,

$O(^1D) + H_2O \rightarrow 2OH$.

Prather

$$\delta[\mathrm{CH_4}](t) \approx +0.995\,\mathrm{e}^{-t/13.6} + 0.005\,\mathrm{e}^{-t/0.285}\ \mathrm{ppb},$$

Prather

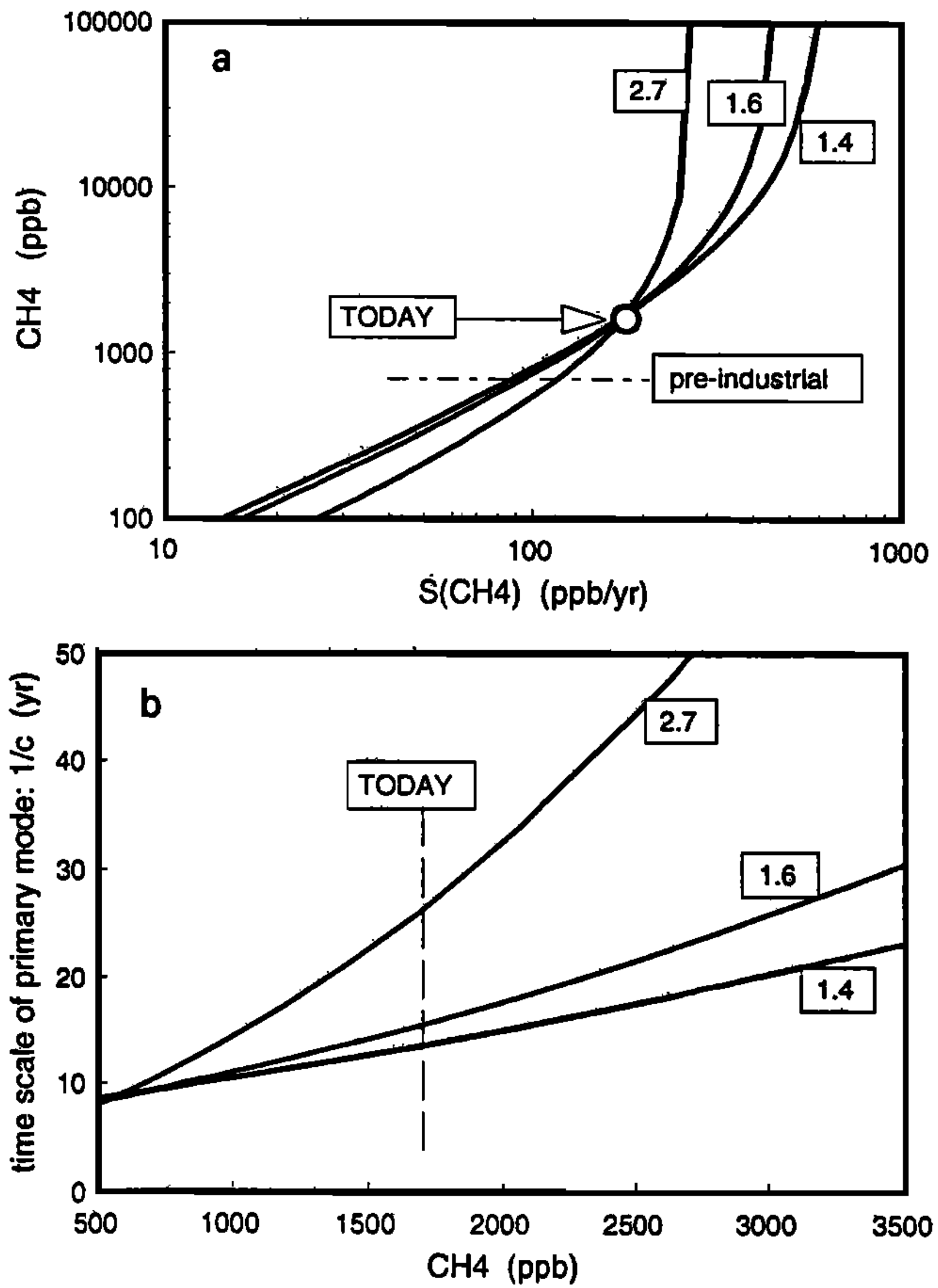

a
100000
10000
1000
100
10
100
1000
CH4 (ppb)
Ṡ(CH4) (ppb/yr)
2.7
1.6
1.4
TODAY
pre-industrial
b
50
40
30
20
10
0
500
1000
1500
2000
2500
3000
3500
time scale of primary mode: 1/c (yr)
CH4 (ppb)
TODAY
2.7
1.6
1.4

Lelieveld et al, 2016

Table 1. Global, annual mean tropospheric source and sink fluxes of OH ($Tmol\,yr^{-1}$). Sources and sinks are also specified for the boundary layer and free troposphere.

Sources/sinks	BL	FT	Troposphere
$O(^1D)+H_2O$	12.5	71.5	84.0 (33 %)
$NO+HO_2$	10.4	66.2	76.6 (30 %)
O_3+HO_2	3.5	30.9	34.4 (14 %)
$H_2O_2+h\nu$	2.3	22.5	24.8 (10 %)
OVOCs, ROOH+$h\nu$	6.6	24.8	31.4 (13 %)
Total OH sources	35.3	215.9	251.2
$OH+HO_y$[1]	4.8	41.4	46.2 (18 %)
$OH+NO_y$[2]	0.8	3.3	4.1 (1.5 %)
$OH+CH_4$	4.1	25.7	29.8 (12 %)
OH+CO	9.6	88.2	97.8 (39 %)
OH+other C_1VOC[3]	5.7	31.3	37.0 (15 %)
OH+C_{2+}VOC[4]	10.3	24.4	34.7 (14 %)
Rest	0.4	1.2	1.6 (0.5 %)
Total OH sinks	35.7	215.5	251.2

[1] H_2, O_3, H_2O_2, radical–radical reactions. [2] NO, NO_2, HNO_2, HNO_3, HNO_4, ammonia, N-reaction products. [3] VOC with one C atom (excl. CH_4), incl. CH_3OH, C_1-reaction products. [4] VOC with ≥ 2 C atoms, C_{2+}-reaction products.

Lelieveld et al, 2016

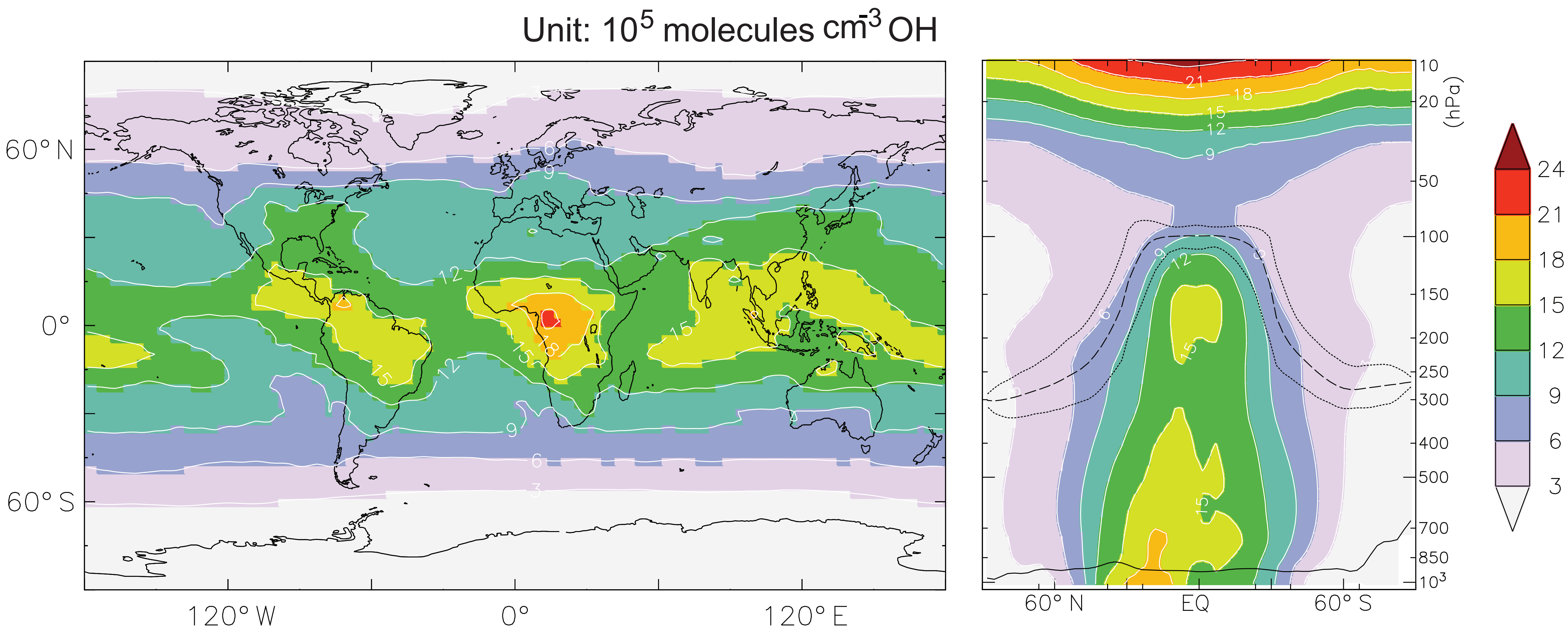

Lelieveld et al, 2016

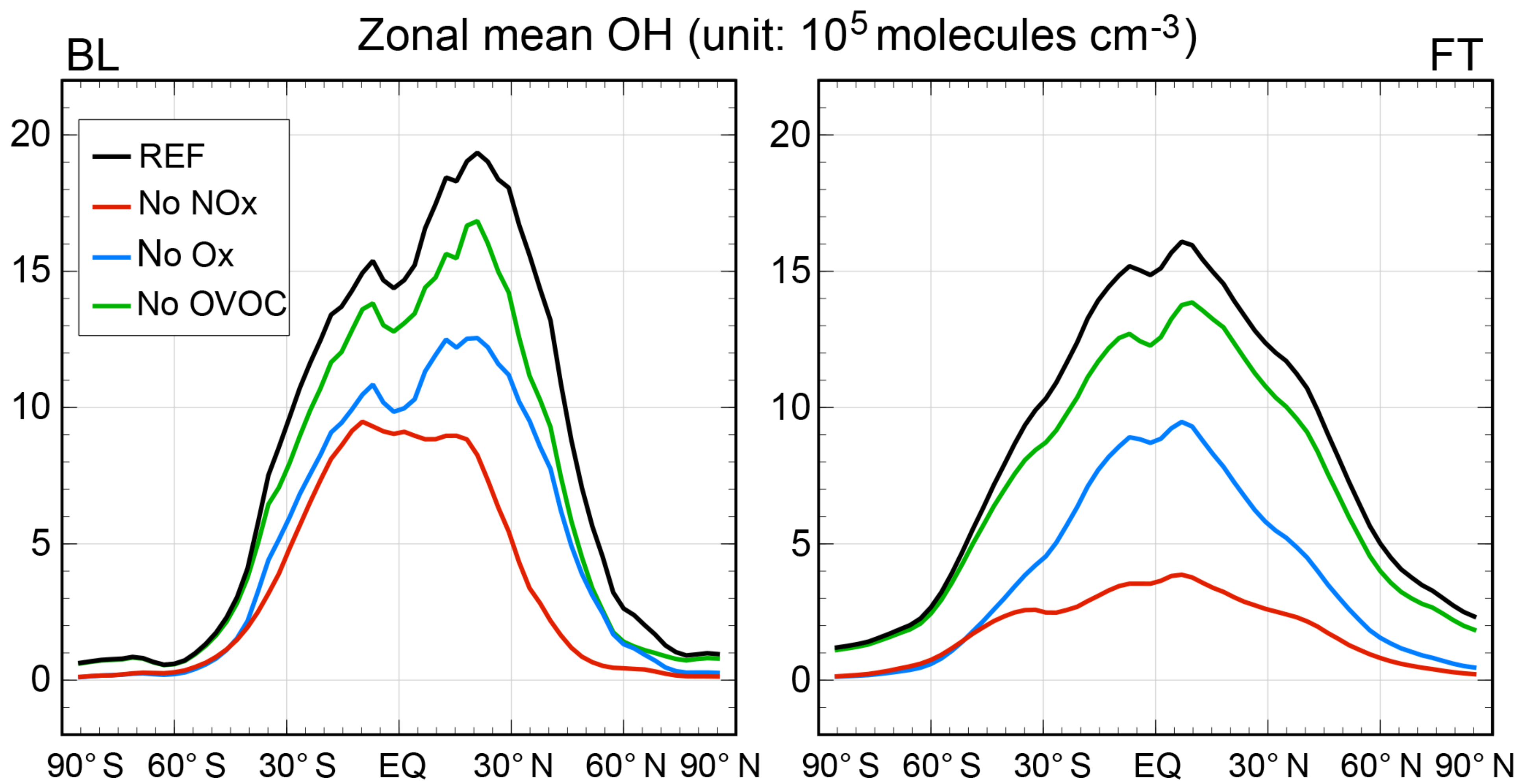

Figure 11. Zonal annual mean OH concentrations calculated in the reference simulation (black) and by successively excluding OH recycling through the NO_x, O_x and OVOC mechanisms.

Table 2. Sensitivity of $\tau_{CH_4 \times OH}$ to climate variables and emissions[a].

Variable [b]	UCI CTM	Oslo CTM3	GEOS-Chem	Literature [c]	Adopted [d]
Chemistry-climate interactions					
Air temperature [e]	−3.9	−2.8	−2.2		−3.0 ± 0.8
Water vapor [e]	−0.32	−0.29	−0.34		−0.32 ± 0.03
Ozone column, 40° S–40° N	+0.66	+0.43[f]	+0.61	+0.28 – 0.76[g] [1] +0.28[h] [2] +0.27[g] [3]	+0.55 ± 0.11
Lightning **NO_x** ***emissions***	−0.14	−0.11	−0.24	-0.08–0.16 [4]	−0.16 ± 0.06
Biomass burning emissions [i]	+0.021	+0.013 +0.003[j]	+0.017		+0.020 ± 0.015
CH_4 abundance [k]	+0.363	+0.307	+0.274	+0.32 [5] +0.28 ± 0.03 [6]	+0.31 ± 0.04 ($f = 1.34 \pm 0.06$)[l]
Convective mass flux	−0.036				N
Optical depth, ice clouds	+0.013				N
Optical depth, water clouds	−0.025			+0.024 [2] −0.075 [3]	N
Anthropogenic emissions					
Land NO_x[m]	−0.15	−0.10	−0.16	−0.137 [5] −0.121 ± 0.055 [7]	−0.14 ± 0.03
Ship NO_x	−0.045	−0.048	−0.017	−0.0412 ± 0.01 [8] −0.0374 ± 0.005 [9] −0.047 [10]	−0.03 ± 0.015
Aviation NO_x				−0.014 ± 0.003 [11]	−0.014 ± 0.003
CO	+0.066	+0.050	+0.065	+0.11 [5] +0.074 ± 0.004 [7]	+0.06 ± 0.02
VOC				+0.047 [5] +0.033 ± 0.01 [7]	+0.04 ± 0.01

[a] Sensitivities are reported as $d\ln(\tau_{CH_4 \times OH})/d\ln(F)$ for each variable F, based on perturbation tests described in Sect. 3.2.

Murray et al, 2013

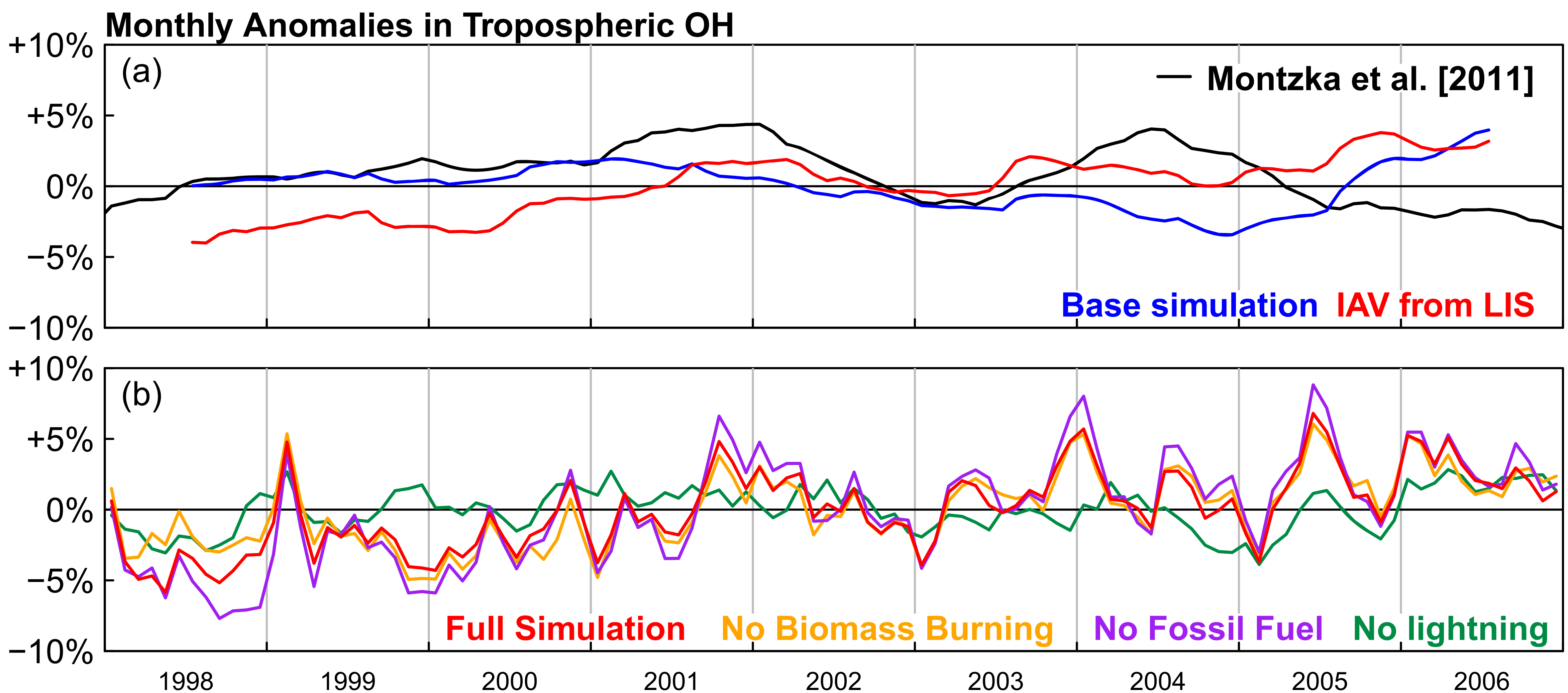

Murray et al, 2013

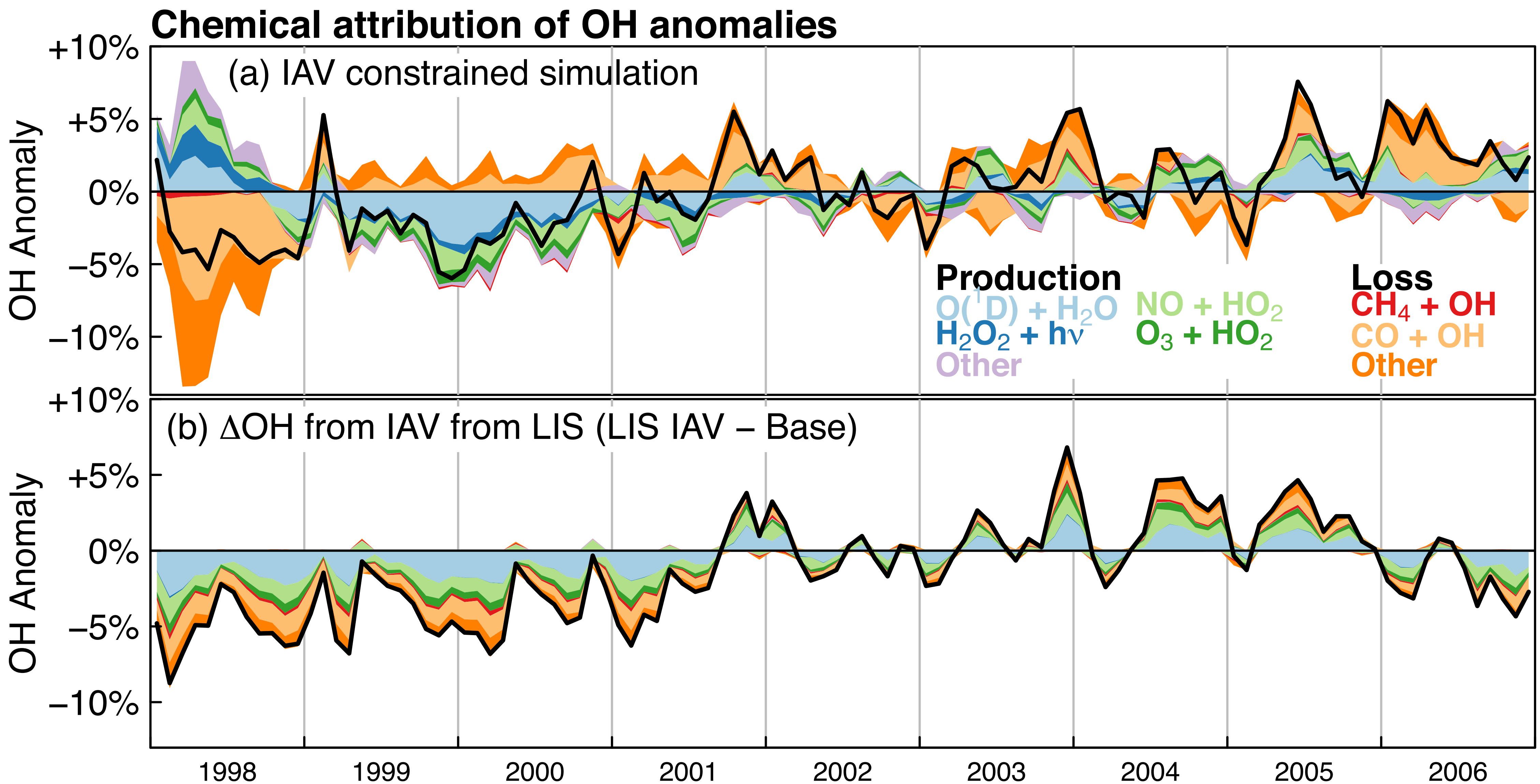

Murray et al, 2013

Table 2. Sensitivity of Simulated IAV in OH to Different Reaction Pathways, Climate Variables, and Emissions

Parameter, P	R With OH Anomalies[a]	Slope of dOH/dP[b] (%/%)	σ in Monthly Anomalies of P[c] (%)
OH anomalies	1.00	+1.00	3.01
Production anomalies	0.32	$+0.97^{+0.17}_{-0.15}$	3.11
Primary production	0.61	$+1.06^{+0.14}_{-0.13}$	2.85
Water vapor	0.14	$+2.89^{+0.58}_{-5.85}$	1.04
Stratospheric ozone	–0.38	$-4.19^{+0.60}_{-0.71}$	0.72
Tropospheric ozone	0.54	$+1.73^{+0.26}_{-0.71}$	2.92
HO_x recycling	0.47	$+0.93^{+0.14}_{-0.12}$	3.25
Loss anomalies	–0.55	$-0.83^{+0.17}_{-0.22}$	3.64
$k_{CH_4+OH}(T)[CH_4]$	–0.63	$-3.67^{+0.53}_{-0.65}$	0.82
$k_{CO+OH}(T)[CO]$	–0.56	$-0.52^{+0.10}_{-0.12}$	5.81
Global emission rates			
Lightning	0.63	$+0.18^{+0.03}_{-0.04}$	16.4
Biomass burning[d]	–0.32	$-0.10^{+0.02}_{-0.03}$	29.5

[a]Pearson correlation coefficient, R, between time series of OH percent anomalies and the forcers.
[b]Slope of reduced major axis (RMA) regression between monthly percent anomalies in OH and the forcers. Range gives 95% confidence intervals calculated from a bootstrap ensemble with 10^3 members.
[c]Standard deviation of monthly percent anomalies in tropospheric mean climate variables, reaction rates, and emissions. All values calculated from the simulation using IAV in lightning from LIS.
[d]Statistics for fire emissions are calculated using time series of NO_x emission; results are very similar for CO emissions, and negative because fires act as a net sink for OH.

Oman et al
Ozone recovery